An R-vine copula analysis of non-ferrous metal futures with application in Value-at-Risk forecasting

An R-vine copula analysis of non-ferrous metal futures with application in Value-at-Risk forecasting

Abstract

We employ the R-vine copula approach to study the dependence structures between non-ferrous metal commodity futures on the London Metal Exchange, focusing on the comparison before and after structural breaks. We find that the center of the dependence structures between non-ferrous metal futures shifts from copper to zinc after the first structural break in 2008 and moves back to copper after the second structural break in 2014. Additionally, we document that non-ferrous metals experienced an increase in the level of integration and tail dependence between 2008 and 2014, while this increase is shown to cease after 2014. We further develop an R-vine copula-based method for forecasting Value-at-Risk, and the backtesting results show superior forecasting accuracy over the benchmark methods. Our study is useful for market participants seeking to enhance their risk management for non-ferrous metals.

Keywords: R-vine copula; dependence structure; financial crisis; Value-at-Risk

JEL classification: C58, G01; L61

1. Introduction

For most economies, non-ferrous metals are vital industrial materials. Due to the wide range of their indispensable industrial applications, the prices of non-ferrous metals have a significant influence on the extraction, processing, and manufacturing sectors (Watkins and McAleer, 2004). In recent years, a significant change has been witnessed in the metal markets. There was a surge in demand for metals in the early 2000s, mainly driven by emerging economies, followed by a market meltdown during the 2008 financial crisis period and a partial recovery following the crisis (Lyócsa et al., 2017). Distinct from other metal classes with which they share common demand factors, non-ferrous metals face an inelastic supply caused by producers' rigid capacity constraints (Scherer and He, 2008). From an economic point of view, an inelastic supply combined with fluctuating demand provides persuasive reasoning as to why one might expect a volatile and complex dependence structure within the non-ferrous metal markets.

Despite its industrial importance, the role of non-ferrous metals in asset allocation remains unclear due to concerns as to the effectiveness of portfolio diversification among non-ferrous metal futures. In other words, whether or not non-ferrous metals as a whole are qualified to be

regarded as a separate asset class remains controversial. Ciner et al. (2020) argue that assets within a separate asset class should demonstrate a high level of integration and a uniform response to common shocks. In view of these features, the dependence structure across non-ferrous metals requires thorough analysis in order to uncover the time-varying patterns of integration among non-ferrous metals, particularly following structural breaks incurred by systematic shocks. Nevertheless, expanding the knowledge base on the dependence structures across non-ferrous metals is undoubtedly vital for hedgers who have physical exposure to these metals, speculators who seek to profit from statistical arbitrage strategy (e.g. pairs trading) across non-ferrous metal markets, as well as policy makers who aim to identify the potential need for regulatory changes (Todorova and Clements, 2018).

Investment within non-ferrous metal commodity futures is being rapidly exploited by index funds, arbitrage traders, and Commodity Trading Advisors (CTAs). Among non-ferrous metal-based investment vehicles, index-tracking exchange-traded funds (ETFs) have received increased attention. Figure 1 shows the predominance of non-ferrous metals index-tracking ETFs in terms of assets under management (AUM). Specifically, index-tracking ETFs are designed to satisfy investors who seek broad exposure to a range of non-ferrous metals. For

example, the PowerShares DB Base Metals Fund (DBB), issued by Invesco, tracks an index composed of futures contracts on multiple non-ferrous metals (DBIQ Optimum Yield Industrial Metals Index). Thus far, its asset

Figure 1: The Total AUM of non-ferrous metal-based ETFs

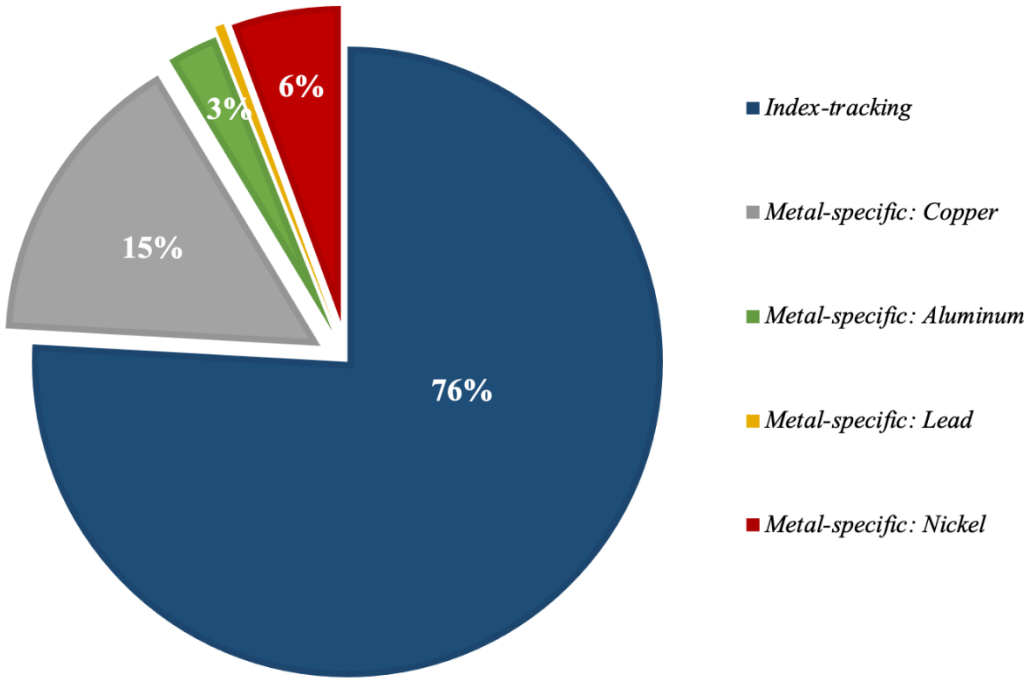

Note: *Index-tracking* denotes the total AUM of all non-ferrous metal index-tracking ETFs, *Metal-specific: Copper* denotes the total AUM of copper ETFs, *Metal-specific: Aluminum* denotes the total AUM of aluminum ETFs, *Metal-specific: Lead* denotes the total AUM of lead ETFs, *Metal-specific: Nickel* denotes the total AUM of nickel ETFs. All data are openly available in *ETF DATABASE* at [https://etfdb.com/etfs/commodity/].

under management (AUM) has reached 86.41 million dollars. Most non-ferrous metal indexes are equal-weighted. ETFs which track these indexes can be regarded as equal-weighted portfolios, constituted by components of the target indexes. However, assessing an index-tracking ETF's Value-at-Risk (VaR) would generate bias, due to the ambiguity of the ETF's

distribution. This ambiguity is rooted in the complexity of the dependence structure across each futures contract in the ETF's portfolio. It is amplified by higher volatilities, non-zero skewness and heavy tails exhibited in commodity futures returns. (Del Brio et al., 2018).

The question of how to efficiently measure the dependence structures between non-ferrous metals is still under debate. To use an analogy, the use of linear correlation or cointegration as a measure of dependence is ultimately an "Achilles' heel" (Liew and Wu, 2013). To address this concern, the copula approach is widely applied in risk management and option pricing. Copula is a multivariate distribution function which is capable of characterizing non-linear dependence structures between financial assets. Copula function defines many new measures which also enable us to deeply exploit dependence in certain extreme scenarios, such as financial crises. However, the types of multivariate copula become increasingly limited as the data dimension expands (Brechmann and Czado, 2013). In addition, a multivariate copula implicitly equips each pair of marginals in a high-dimensional dataset with the same dependence structure, which fails to model the heterogeneity in the dependence structure across pairs of marginals (McNeil and Neslehova, 2009). Based on these drawbacks, Bedford and Cooke (2002) develop a new multivariate copula approach, the so-called vine-copulas. By

appealing to the pair-copula construction (PCC) method (Aas et al., 2009), the vine-copula approach is able to independently capture each bivariate dependence structure by constructing a multi-level tree. Moreover, Nagler and Czado (2016) develop a nonparametric method, which can overcome the "curse of dimensionality" in vine-copula parameter estimations. In this respect, the vine-copula approach is both more flexible and efficient in contrast to the multivariate copula approach. Thus, we employ the vine-copula approach in our research.

Based on these lines of interest, it is worthwhile investigating the dependence structure between non-ferrous metal futures, in particular, to reveal the change that occurs following structural breaks. In this paper, we use the R-vine copula approach to study the dependence structures between major non-ferrous metal futures on the London Metal Exchange (LME), before and after structural breaks. We select five futures contracts traded in the LME, namely aluminum, copper, nickel, zinc, and lead. These metal futures have large trading volumes, and their underlying metals are widely used for industrial purposes. We find that the core of non-ferrous metal futures, which is characterized by the non-ferrous metal that has the strongest dependence on the other four futures, shifts from copper to zinc after the first structural break and moves back to copper after the second structural break. The diversification benefit among

major non-ferrous metal futures diminishes after the first structural break and increases after the second structural break. Accordingly, we confirm the increasing presence of lower tail dependence between the five non-ferrous metal futures after the first structural break. However, this pattern disappears after the second structural break. Based on Nikoloulopoulos et al. (2012), we also develop an R-vine copula-based VaR forecasting scheme and the backtesting confirms its merits over other benchmark methods.

This study contributes to the literature in three ways. First, we investigate the dependence structures between non-ferrous metal futures traded in the LME focusing on analyzing the change after structure breaks. This is an area of research which has received little attention in previous studies. Second, based on the R-vine copula analysis, we provide further evidence of a reduction in the diversification benefit among non-ferrous metals between 2008 and 2014. This complements the existing findings that fewer diversification benefits are detected in other types of markets after the financial crisis (Gerlach et al. 2006; Lu et al. 2012 and Silvennoinena and Thorp 2013). Third, the backtesting results for VaR forecasting show superior accuracy over benchmark methods before and after two structural breaks. Our study expands on the limited knowledge on non-metal futures, while the VaR forecasting scheme we developed,

combined with the statistical tests on structural breaks, may help to improve the risk management ability of index-tracking ETFs, CTAs, and arbitrage traders in non-ferrous metal markets, thus being of value to other investors, spot market participants, and market regulators.

This paper is organized as follows: Section 2 reviews the relevant literature, Section 3 explains the methodology, and Section 4 describes our dataset and discusses the results of the structural break testing and marginal distribution modelling. Section 5 analyzes the dependence structure results in depth. Section 6 interprets the VaR forecasting and backtesting results. Section 7 concludes the paper.

2. Literature Review

Many studies have focused on dependence and volatility across spot metal markets and futures markets. Choi and Hammoudeh (2010) confirm increasing correlations between spot markets of Brent oil, WTI oil, copper, gold, and silver. Specifically, Ciner (2001) finds no evidence of cointegration between gold and silver futures traded in Japan. Sensoy (2013) further documents that there is no significant impact on the volatility levels of gold and silver during the turbulent year of 2008. In contrast, Xu and Fung (2005) suggest a strong cross-

market volatility spillover effect in gold, silver and platinum futures across U.S. and Japanese markets. A detailed review of studies on dependence and volatility across metals has been produced by Vigne et al. (2017)

The copula approach has been widely applied to multiple fields in finance and econometrics (e.g. Embrechts 1999; Longin and Solnik 2001; Patton 2002; Patton 2006; Low et al. 2013). Early studies such as Junker and May (2005) and Nelsen (2006) mainly focus on the ability of bivariate copula in modelling two-dimensional dependence. However, the rapidly growing quantity of financial data has highlighted the superior ability of the vine copula approach in modelling high-dimensional dependence. A strand of literature aims to employ the vine-copula approach to explore a variety of dependence types, such as intra-market dependence (e.g. So and Yeung 2014; Abbara 2014; Markwat 2014), cross-market dependence (e.g. Ning 2010), inter- and intra-continental dependence (e.g. Huang and Ning 2017) and dependence within a supply chain (e.g. Pircalabu and Jung (2017) etc. Another strand of literature aims at identifying the time-varying pattern of the dependence via the vine-copula approach, particularly during a period of financial crisis (e.g. Zhang 2014; Huang and Ning 2017). Moreover, recent studies also attempt to combine several cutting-edge methods in

finance and econometrics using copula to improve the performance of dependence modelling. For example, Mensi et al. (2017) develop a wavelet-based copula method to examine dependence structures between several commodity futures with implied volatility indexes. Tiwari et al. (2020) employ a time-varying market switching copula model to study dependence dynamics between gold and oil prices.

VaR forecasting based on vine-copula has received increasing levels of attention in recent years. The results of previous studies that have adopted the copula approach to improve the accuracy of Value-at-Risk forecasting demonstrate its superior performance. (see e.g. Lu et al. 2011; Nikoloulopoulos et al. 2012; Siburg et al. 2015; Weiss and Supper 2013; Zhang et al. 2014 and references therein). It is noteworthy that Zhang et al. (2014) use C-vine, D-vine and R-vine copula to model the internal structures of 10 international stock indices and forecast their portfolio's Value at Risk (VaR) and Expected Shortfall (ES). The backtesting results of VaR forecasting with three kinds of vine copula show sufficient accuracy. Yang et al. (2019) employ realized volatility to characterize dependence structure and risk spillover and implement a copula approach to calculate Conditional Value-at-Risk (CoVaR) and Conditional Expected Shortfall (CoES). Li and Wei (2018) combine the variational mode decomposition

(VMD) method with a copula approach to analyze conditional VaR (CoVaR) and delta CoVaR (ΔCoVaR) between oil and the stock market.

3. Methodology

3.1. Structural break test

We employ a modified version of the statistical test developed by Kojadinovic et al. (2015) to detect structural breaks for Kendall's τ in multivariate time series.[1] N denotes the number of commodity futures studied and T denotes the sample size. The log-returns of commodity futures constitutes an $\mathbb{R}^N$-valued multivariate time series $\boldsymbol{R} = (\boldsymbol{R_1}, \boldsymbol{R_2}, \cdots, \boldsymbol{R_T})$. The statistical procedure builds on a general framework, whereby the null hypothesis aims to test whether $\boldsymbol{R}$ has a constant conditional distribution function (CDF) $\boldsymbol{F}$ over time. i.e.

$$\mathrm{H}_0\text{: } \exists\, \boldsymbol{F} \text{ such that } \boldsymbol{R_1}, \boldsymbol{R_2}, \cdots, \boldsymbol{R_T} \text{ have c.d.f. } \boldsymbol{F}$$

in contrast with the alternative hypothesis H_A indicating the non-constancy of CDF. over time.

Following Kojadinovic et al. (2015), a generalized test statistic for H_0 is

$$S_T = \max_{2 \le t \le T-2} \left| \sqrt{T}\, \gamma(t, T) \left(U_{m,1:t}(\boldsymbol{R}) - U_{m,t:T}(\boldsymbol{R}) \right) \right| \qquad (1)$$

[1] The original test of Kojadinovic et al. (2015) is designed to detect structural breaks in Spearman's rho.

where $\gamma(t,T) = \frac{t(T-t)}{T}$ and $U_{m,t_1:t_2}(\boldsymbol{R}) = \frac{2\sum_{t_1 \le i \le j \le t_2} m(\boldsymbol{R_i},\boldsymbol{R_j})}{(t_2-t_1+1)(t_2-t_1)}$ for $1 \le t_1 \le t_2 \le T$.

We emphasize that the change in the joint distribution function $\boldsymbol{F}$ may be invoked by the change in the moments of $\boldsymbol{F}$, such as change in the mean and variance, as well as by the change in the multidimensional dependence measured by Kendall's τ. According to Bücher et al. (2016), we can further detect whether the change of $\boldsymbol{F}$ is incurred by changes in the moments or structural breaks in Kendall's τ via the appropriate selection of $m(\boldsymbol{R_i}, \boldsymbol{R_j})$. Thus, for any $1 \le i \le j \le T$, we choose $m(\boldsymbol{R_i}, \boldsymbol{R_j}) = \mathrm{I}(\boldsymbol{R_i} > \boldsymbol{R_j}) + \mathrm{I}(\boldsymbol{R_i} < \boldsymbol{R_j})$ to allow tests for H_0 particularly sensitive to structural breaks in the Kendall's τ of $\boldsymbol{R}$. Under the null hypothesis H_0 and some regular conditions (see Bücher et al. 2016 for details), we have

$$S_T \xrightarrow{d} 2\sigma_{m_1} \sup_{s\in[0,1]} |\boldsymbol{\mathcal{B}}(s) - s\boldsymbol{\mathcal{B}}(1)| \tag{2}$$

where $\boldsymbol{\mathcal{B}}(\cdot)$ denotes a Brownian motion and the long run variance

$$\sigma_{m_1}^2 = \mathrm{E}(m_1(\boldsymbol{R_1})^2) + 2\sum_{i=2}^{\infty} \mathrm{E}[m_1(\boldsymbol{R_1})m_1(\boldsymbol{R_i})] \tag{3}$$

with $m_1(\boldsymbol{x}) = \mathrm{E}[m(\boldsymbol{x}, \widehat{\boldsymbol{R}}_{\boldsymbol{1}}) - m(\widehat{\boldsymbol{R}}_{\boldsymbol{1}}, \widetilde{\boldsymbol{R}}_{\boldsymbol{1}})]$ for any $\boldsymbol{x} \in \mathbb{R}^N$ and $\widehat{\boldsymbol{R}}_{\boldsymbol{1}}, \widetilde{\boldsymbol{R}}_{\boldsymbol{1}}$ indicating two independent random vectors that have the same distribution as $\boldsymbol{R_1}$.

3.2. Marginal distribution modelling

It is well known that financial time series typically exhibits autocorrelations and heteroscedasticity (Francq and Zakoian, 2019). As the copula analysis requires *i.i.d.* samples, a common choice is to apply an ARMA-GARCH model to remove autocorrelations and heteroscedasticity in financial time series to facilitate copula analysis (see Lu et al. (2014) and Apergis et al. (2020) and references therein). Moreover, Bollerslev (1987) emphasizes that leptokurtosis in financial time series could be more effectively captured by fitting the GARCH errors with Student's *t* innovations. Therefore, we employ the GARCH (1,1) model with Student's *t* distributed innovations for the marginal model[2]:

$$R_{\mathrm{i,t}} = \mu_i + \sigma_{i,t}\varepsilon_{i,t} \tag{4}$$

$$\sigma_{i,t}^2 = \omega_i + \alpha_i R_{i,t-1} + \beta_i \sigma_{i,t-1}^2 \qquad i = 1, \dots, N, \quad t = 1, \dots, T \tag{5}$$

where $R_{\mathrm{i,t}}$ denotes the log-return of futures contract i in time t, N denotes the number of commodity futures studied, T denotes the sample size, and $\varepsilon_{i,t}$ follows Student's t distribution with ν_i degree of freedom.

[2] GARCH (1,1) model is an adequate model for our data according to the evidence from the autocorrelation and heteroscedasticity tests. Higher orders of both ARMA and GARCH models have experimented and there is no significant difference in the results.

After marginal distribution modelling, we need to re-examine the autocorrelations, heteroscedasticity, as well as the leverage effect to verify the existence of (approximately) *i.i.d.* standardized residuals, which are essential for the validity of copula analysis. The leverage effect is proposed to account for the asymmetry response of the volatility in relation to innovations in financial time series. Since Francq and Zakoian (2019) find the joint existence of heteroscedasticity, autocorrelation, and leverage effect in the sequence of the financial returns, the residuals derived from the marginal model are simultaneously verified by the Ljung-Box test (Ljung and Box 1978), the Lagrange Multiplier (LM) test (Engle 1982) and the Sign Bias test (Engle and Victor, 1993) which detect autocorrelations, heteroscedasticity and leverage effect, respectively.

3.3. Vine-copula approach

A copula is a multidimensional joint distribution function whose marginal is uniformly distributed on [0,1]. Sklar's theorem endows a copula with the capacity to capture dependence structures. However, a single copula function can only characterize the dependence structure for two random variables. When the dimension is higher than two, a multivariate copula can

be used, however it forces the same dependence structure for each pair of random variables. This defect greatly restricts the ability of multivariate copula to capture multidimensional dependence structures.

In principle, this approach decomposes a multivariate density function into the product of the marginal densities and a series of unconditional or conditional pair-copulas. Furthermore, various kinds of pair-copula families can be chosen to model the dependence of each pair of random variables. The construction of vine-copula models is diverse due to the different types of connections between nodes and edges and the different progressive relationships of tree structures. Bedford and Cooke (2002) proposed a graphical construction approach: the regular vine (R-vine). In this approach, the tree structure of each level is different. The nodes in each tree are connected through the edges, and each node comes from a specific edge in the previous tree. An edge only connects two nodes in each tree if they share a common node in the previous tree (proximity condition). A pair-copula characterizes paired random variables that correspond to each edge.

Using the vine-copula approach to decompose n-dimensional random vectors $X_n = (X_1, X_2, \dots, X_n)$ will generate $n-1$ tree structures and $n \times (n-1)$ pairs of random

variables that need to be characterized by pair-copula functions. If $f(x_1, x_2, \dots, x_n)$ denotes the joint density function of this random vector, the R-vine decomposition of the joint density function is as follows:

$$f(x_1, x_2, \dots, x_n) = \prod_{i=1}^{n} f(x_i) \prod_{i=1}^{n-1} \prod_{e \in E_i} c_{j_e, k_e | d_e} \{F(j_e | d_e), F(k_e | d_e); d_e\} \quad (6)$$

where $f(x_k), k = 1,2, \dots, n$ denotes the marginal density of X_n, $c_{j_e, k_e | d_e}(\cdot, \cdot)$ represents the pair-copula density corresponding to edge e which connects nodes j and k in the i^{th} tree, and E_i is a set that consists of all edges in the ith tree. $d_e = \mathrm{A}_j \cap A_k$, where A_j and $A_k$are two sets of nodes in the first tree that are reachable by nodes j and k, $j_e = \mathrm{A}_j - d_e$, $k_e = \mathrm{A}_k - d_e$. The second product symbol takes all $n - 1$ trees, while the third product symbol takes all $n - j$ pair-copula functions in the i^{th} tree.

Each bivariate copula in vine-copula depends on two conditional cumulative distribution functions (CDF): $F(j_e | d_e)$, $F(k_e | d_e)$ and conditioning variables in d_e. The number of variables in d_e increases when the tree level increases, which makes each bivariate copula a $|d_e| + 2$ dimensional function to be estimated. Haff et al. (2010) suggest that it may still be possible to estimate a bivariate copula that depends additionally on the single conditioning

variable, using some sort of smoothing technique. However, at higher levels, this becomes difficult in a parametric setting and impossible in a non-parametric one. To make fast, flexible, and robust inferences, one must assume that each bivariate copula in a vine copula construction is independent of the conditioning variables. i.e.

$$c_{j_e,k_e|d_e}\{F(j_e|d_e), F(k_e|d_e); d_e\} = c_{j_e,k_e|d_e}\{F(j_e|d_e), F(k_e|d_e)\} \quad (7)$$

This is the simplifying assumption. Following Kurz and Spanhel (2017), we implement a constant conditional correlation (CCC) test to check whether the simplifying assumption can be relaxed in our data Technical details relating to the test are provided in Appendix A.

3.4. Selection and estimation for R-vine copula

The following three steps are necessary for fitting an R-vine copula specification to a given high-dimensional dataset:

(1) Select a specific R-vine copula structure.

(2) Select the appropriate pair-copula family for each pair in the selected R-vine-copula structure.

(3) Estimate the parameter(s) for each copula.

The ideal method is to repeat steps (2) and (3) for every possible R-vine copula structure. However, n-dimensional random variables may have $\binom{n}{2} \times (n-2)! \times 2^{\binom{n-2}{2}}$ possible R-vine copula structures (Morales-Napoles et al., 2010). Compared to the number of dimensions, the rapidly expanding number of R-vine copula structures makes the ideal method inefficient.

We therefore use a sequential estimation method proposed by Dißmann et al. (2013). Dißmann et al. (2013) demonstrate that the copula families specified in the first tree of the R-vine often have the greatest influence on the model fit. Joe et al. (2010) also stated that, in order for a vine-copula to show dependency for all bivariate margins, it is sufficient for the bivariate copulas in the first tree to display a dependence. Thus, the stronger the dependence that the first tree structure can capture, the more independent the transform variables in the subsequent tree structures are. Whether the first tree structure can fully capture the strongest dependence structure between variables is of vital importance. Based on these arguments, this method should be conducted from the first tree structure and steps (1), (2) and (3) repeated for each tree structure sequentially. Based on certain dependence measures, this method employs the maximum spanning tree (MST) algorithm as the selection criteria for the first tree and

subsequent tree structures. In other words, the tree structure that solves the following optimization problem is selected:

$$\max_{t_i \in T_i} \sum_{\substack{edges\ e=\{i,j\} in \\ spanning\ tree\ t_i}} \left|\delta_{i,\mathrm{j}}\right| \quad , \mathrm{i} \neq \mathrm{j} \tag{8}$$

where T_i is a collection of all possible tree structures in the i^{th} tree, t_i denotes a specific i^{th} tree structure, e is an arbitrary edge in tree t_i, and $\delta_{i,j}$ is the dependence measure's value between a pair of random variables corresponding to edge e. In this study, we use the Kendall's τ as dependence measure $\delta_{\mathrm{i,j}}$ in the MST algorithm.

After the tree structure selection, we need to select an appropriate pair-copula family for each pair of random variables in this tree. Two approaches are widely used as selection criteria for pair-copulas: the copula goodness-of-fit test and the Akaike Information Criterion (AIC). Manner (2007) finds that, compared with the copula goodness-of-fit test, the AIC are more reliable in pair-copula selection. Therefore, we use the AIC as the pair-copula selection criterion.

Finally, we apply the maximum likelihood estimation to estimate the parameters of each specified pair-copula in the corresponding tree. After parameter estimation, the transformed

variables used as input parameters for the next trees are obtained using the $h(\cdot)$ function (Aas et al., 2009; Dißmann et al., 2013). The tree-wise selection and estimation procedure described here give sequential estimates of pair-copula parameters, which are quite quickly obtained and can be used as starting values for a full maximum likelihood estimation (Aas et al. 2009; Hobæk and Haff 2010). Since most of the pair-copula families can model the independence well, this method also reduces the difficulty of fitting high order tree structures. In addition to this, the sequential estimation can minimize rounding errors caused by high-order tree structures (Brechmann and Czado 2013). Our implementation is based on R packages "VineCopula" (Nagler et al., 2019) and "pacotest" (Kurz, 2019).

3.5. Value-at-risk forecasting

In order to shed light on the risk management of investors in non-ferrous metal markets, we employ an out-of-sample VaR forecasting procedure developed by Nikoloulopoulos et al. (2012). Recall that N is the number of metal commodity futures we considered, T is the sample size, and K is the repetition time of simulation. The procedure can be summarized in the following steps:

(1) We use the first 60% of the sample as the in-sample period[3]. For each $i = 1,2,\dots,N$, the first 60% of the return sequence, i.e. $\{R_1^{(i)}, R_2^{(i)}, \dots, R_\tau^{(i)}\}$, $\tau = 0.6 \times T$, is filtered by the marginal model to obtain approximately $i.i.d.$ residual sequences: $\{\varepsilon_1^{(i)}, \varepsilon_2^{(i)}, \dots, \varepsilon_\tau^{(i)}\}$.

(2) For each $i = 1,2,\dots,N$, convert standardized residual sequences into unit intervals by the empirical Probability Integral Transform (PIT) method. Denote the $[0,1]$ variables by $\{u_t^{(i)}, 1 \le t \le \tau\}, i = 1,2,\dots,N$.

(3) Use the R-vine copula approach to model high dimensional dependencies across different scaled sequences.

(4) For each $i = 1,2,\dots,N$, $\{u_{1,\tau+1}^{(i)}, u_{2,\tau+1}^{(i)}, \dots, u_{K,\tau+1}^{(i)}\}$ is obtained from simulating observations K times from the R-vine copula specification in step (3) using the algorithms of Aas et al (2009).

(5) For each $i = 1,2,\dots,N$, convert $\{u_{j,\tau+1}^{(i)}, 1 \le j \le K\}$ to $\{\varepsilon_{j,\tau+1}^{(i)}, 1 \le j \le K\}$, use the quantile functions of the Student's *t* distribution.

(6) For each $i = 1,2,\dots,N$, forecast one step ahead $\hat{\sigma}_{\tau+1}^{(i)}$ and $\hat{\mu}_{\tau+1}^{(i)}$ from the marginal model specification in step (1), then compute $\{R_{j,\tau+1}^{(i)}, 1 \le \mathrm{j} \le \mathrm{K}\}$ using the following equation:

[3] Another proportion that yields similar results has also been tried.

$$R_{j,\tau+1}^{(i)} = \hat{\mu}_{\tau+1}^{(i)} + \hat{\sigma}_{\tau+1}^{(i)} \cdot \varepsilon_{j,\tau+1}^{(i)}, \qquad 1 \le j \le K,\ 1 \le i \le N \tag{9}$$

(7) For each $i = 1,2,\dots,N$, construct an equal-weighted portfolio and compute the portfolio returns according to the following equation:

$$R_{j,\tau+1} = \frac{1}{N}\sum_{i=1}^{N} R_{j,\tau+1}^{(i)}, \qquad 1 \le j \le K,\ 1 \le i \le N \tag{10}$$

(8) For $q \in \{0.01, 0.05, 0.1\}$, calculate the q^{th} quantile $R_{\tau+1}(q)$ for $\{R_{j,\tau+1}, 1 \le$ j ≤ K}. Then $VaR_{\tau+1}^{q} = -R_{\tau+1}(q)$ is the Value-at-Risk.

(9) We use a rolling window scheme (i.e. the length of the in-sample period is fixed to $0.6 \times T$, the start and the end of the in-sample period moves 1 step ahead simultaneously) and repeat Step (1)-(8) to produce a 1-step-ahead forecast for each time point in the out-of-sample data.

3.6. Value-at-Risk Backtesting

Let $\{R_t, \tau + 1 \le t \le T\}$ denote the realized returns in the VaR forecasting period, where τ and T are defined in Section 3.4. For any $\tau + 1 \le t \le T$, define an indicator function:

$$I_t = \begin{cases} 1, & R_t < -VaR_t^q \\ 0, & R_t \ge -VaR_t^q \end{cases} \tag{11}$$

$I_t = 1$ means the occurrence of a violation. In theory, $P(I_t = 1) = P\left(R_t < -VaR_t^q\right) = q$ and $P(I_t = 0) = P\left(R_t \geq -VaR_t^q\right) = 1 - q$, therefore q also represents the theoretical violation rate, which is defined in step (8) in Section 3.4. Moreover, the partial sum $Z_n = \sum_{t=\tau+1}^{n} I_t$ is binomially distributed with $P(Z_n = k) = C_n^k q^k (1-q)^{n-\tau-k}$ where $1 \leq k \leq n,\ \tau + 1 \leq n \leq T$.

We employ two types of VaR backtesting methods: the unconditional coverage test (UC test) and the conditional coverage test (CC test) proposed by Christoffersen (1998) and Christoffersen and Pelletier (2004), respectively, to evaluate the out-of-sample forecast accuracy of our VaR forecasting scheme.

The unconditional coverage test is the log-likelihood ratio test with the following test statistic:

$$LR_{uc} = -2\log\frac{P(Z_T = M; q)}{P(Z_T = M; q_e)} = -2\log\frac{q^M(1-q)^{T-\tau-M}}{{q_e}^M(1-q_e)^{T-\tau-M}} \tag{12}$$

where M is the number of violations in $T - \tau$ samples and q_e is the empirical violation rate, i.e. $q_e = M/(T-\tau)$. The unconditional coverage test only considers the number of violations

in the test sequence, whereas the conditional coverage test accounts for both the number and order of violations in the test sequence.

The conditional coverage test is also the log-likelihood ratio test, and the test statistic LR_{cc} has the following form:

$$LR_{cc} = -2\log\frac{P(Z_T = M; q)}{P(Z_T = n_{01} + n_{11}; q_{01}, q_{11})} = -2\log\frac{q^M(1-q)^{T-\tau-M}}{{q_{01}}^{n_{01}}(1-q_{01})^{n_{00}}{q_{11}}^{n_{11}}(1-q_{11})^{n_{10}}} \quad (13)$$

where $q_{ij} = P(I_t = j|I_{t-1} = i)$, $n_{ij} = (T-\tau)\, q_{ij}$, $i,j = 0,1$, $M = n_{01} + n_{11} + n_{00} + n_{10}$ is the number of violations in $T-\tau$ samples, and q is the theoretical violation rate. Under the null hypothesis, the limiting distribution of LR_{cc} and LR_{uc} are given below:

$$LR_{uc} \xrightarrow{d} \chi_1^2 \quad and \quad LR_{cc} \xrightarrow{d} \chi_2^2 \ , \qquad n \to \infty \quad (14)$$

The null hypothesis is that the test sequence shows serial independence with violation rate q. Since the conditional coverage test is a mixed statistical test, it is designed to jointly test both the exceedance and the independence in an observed sequence.

4. Data and preliminary results

4.1. Data and Results for structural break testing

The literature documenting evidence of the weekend effect in various commodity spot and futures markets is extensive (e.g. Gay and Kim, 1987; Chang and Kim, 1988; Singal and Tayal, 2019). The weekend effect is defined as Friday's return minus the following Monday's return (Chen and Singal, 2003), which can add noise to the daily return of commodity futures and reduce the effectiveness of marginal distribution modelling. We therefore use the log-return of weekly settlement prices[4] of five major non-ferrous metal commodity futures, namely aluminum, copper, nickel, zinc and lead in the London Metal Exchange (LME). These metal futures have large trading volumes, and their underlying metal commodities are widely used for industrial purposes. For example, aluminum is broadly used in transportation and packaging due to its low density, and copper is mainly used to produce electrical wire and cable due to its high conductivity. LME offers a sizable platform where worldwide participants and investors, involved in the non-ferrous metal markets, can hedge against the risk arising from price fluctuation or seek to broaden their exposure to non-ferrous metals (Watkins and McAleer 2006). LME is also the world's largest international trading center for non-ferrous metals. For instance, approximately 95% of the total world trade in copper futures occurs through the LME.

[4] We do not use daily data because it tends to be much noisier and contains the weekend effect.

Our data was downloaded from DataStream, and the sample period starts from January 1, 2002 to December 27, 2019.[5] The period covers the global financial crisis in 2008 and the European sovereign debt crisis in 2010, which may incur multiple structural breaks in the dependence structure. Following Inclan and George (1994), we utilize a binary segmentation scheme based on the structural break test described in Section 3.1 to iteratively detect multiple change points for Kendall's tau in our data. The test results suggest that the sample has two structural breaks. The first structural break occurs at August 22, 2008 and the second structural break occurs at January 31, 2014. The identification of structural breaks enables us to study the dependence structures between the five major non-ferrous metal futures, in particular, the variation in the dependence before and after structure breaks. Thus, we separate the sample into three periods:

- **Period 1** is from January 1, 2002, to August 22, 2008, and represents the period before the first structural break.
- **Period 2** covers from August 22, 2008, to January 31, 2014, and represents the period between the first structural break and the second structural break.
- **Period 3** spans from January 31, 2014, to December 31, 2019, and represents the period after the second structural break.

[5] We choose not to include the samples in 2020 due to the significant impact of COVID-19, which we will investigate in the future.

4.2. Descriptive statistics and marginal distribution modelling

Table 1 summarizes the descriptive statistics for the weekly log-returns in the three periods. The log-returns of five non-ferrous metal futures present leptokurtosis in all three periods. Correspondingly, in most cases, the Jarque-Bera test for each non-ferrous metal futures indicates non-normality. The extreme values of the log-returns of non-ferrous metal futures in Period 2 are generally greater than those in Period 1. However, the extreme values in Period 3 decrease in contrast to those in Period 2. This evidence tentatively implies that the extent of the impact of the "tail events" on the European non-ferrous metal increases after the first structural break and decreases after the second structural break.

The residuals derive from the GARCH (1,1) model, which we chose to fit with marginal distributions, have passed all diagnostic checks, including the Lagrange Multiplier test, the Ljung-Box test and the Sign Bias test in all three periods. This indicates that we have successfully obtained approximately *i.i.d.* residuals and there is no need to further employ asymmetrical GARCH models to improve the marginal distribution modelling. We also test the Goodness-of-Fit of Student's *t* distribution to the innovations of marginals. We find that

the Student's *t* distributed model is a suitable model for marginal distributions. One can refer to Appendix D for detailed results and analysis on marginal distribution modelling.

Table 1. Descriptive statistics for weekly log-returns of five non-ferrous metal futures

	***Period 1**: Jan, 2002-Aug, 2008*							
	Num.	**Min**	**Max**	**Mean**	**Std.Dev.**	**Skew**	**Kurtosis**	***p*-value**
Al	345	-13.48	7.22	0.22	2.9	-0.56	1.62	0.0000
CU	345	-13.89	10.39	0.47	3.62	-0.46	1.06	0.0000
NIC	345	-19.97	13.82	0.34	5.23	-0.23	0.43	0.0526
ZINC	345	-17.27	16.09	0.22	4.62	-0.19	1.2	0.0000
LEAD	345	-16.95	23.35	0.4	5.08	-0.29	2.15	0.0000
	***Period 2**: Aug, 2008-Jan, 2014*							
	Num.	**Min**	**Max**	**Mean**	**Std.Dev.**	**Skew**	**Kurtosis**	***p*-value**
Al	283	-16.49	9.57	-0.15	3.58	-0.33	1.52	0.0000
CU	283	-24.45	13.48	0.00	4.59	-1.22	5.74	0.0000
NIC	283	-22.31	32.01	-0.09	5.68	0.34	4.48	0.0000
ZINC	283	-17.75	11.46	0.08	4.61	-0.38	1.15	0.0000
LEAD	283	-19.09	22.34	0.09	5.41	-0.04	1.59	0.0000
	***Period 3**: Jan, 2014-Dec, 2019*							
	Num.	**Min**	**Max**	**Mean**	**Std.Dev.**	**Skew**	**Kurtosis**	***p*-value**
Al	308	-10.96	11.89	0.01	2.49	0.39	2.26	0.0000
CU	308	-6.28	10.61	-0.05	2.51	0.49	0.91	0.0000
NIC	308	-10.6	13.54	0.00	3.92	0.28	0.04	0.1213
ZINC	308	-7.16	10.47	0.05	3.03	0.21	0.07	0.3006
LEAD	308	-10.42	11.73	-0.04	3.00	0.35	1.57	0.0000

Note: **AL**: Aluminum, **CU**: Copper, **NIC**: Nickel, **ZINC**: Zinc, **LEAD**: Lead. ***p*-value** denotes the *p*-value of the Jarque-Bera test. **Num.** is the number of observations. **Min /Max** denote the minimum or maximum value over the sample period. **Mean** is the mean value over the sample period. **Std.Dev.** represents standard deviation of the sample. **Skew/ Kurtosis** denote skewness or leptokurtosis of the sample respectively.

5. Dependence structure results

In this section, we employ the R-vine copula to investigate the dependence structure between the non-ferrous metal futures we have considered in this paper, with a focus on studying the change after the structural breaks.

Note that the simplifying assumption can overcome the curse of dimensionality in vine-copula's parameter estimation and can make inferences fast, flexible, and robust (Haff et al. 2010). Before analyzing the dependence structure, we employ the CCC test to examine whether the simplifying assumption holds for each conditional bivariate copula in the vine copula. The results of the CCC test show that the simplifying assumption cannot be rejected in all three high-level tree structures at the 5% significance level in the three periods.

Dißmann et al. (2013) highlights that most dependencies between marginal variables are specified in the first tree of R-vine. In light of this salient feature, the first tree structure of the R-vine copula in Period 1, Period 2 and Period 3 are displayed in Figures 2, Figure 3, and Figure 4, respectively. In the following section, we focus on discussing and comparing the dependence structure in the first tree of R-vine, before and after the structural breaks. The remaining tree structures, modeled by the R-vine copula in three periods, are listed in Table 2.

5.1. The dependence structure before the first structural break

As shown in Figure 2, we can observe that there are three of four edges connected to copper in the first tree, while copper is not directly connected with lead. Thus, copper has the strongest impact on the dependence structure of the five futures before the first structural break, which can be regarded as the core of metal futures in their dependence structure. The indices of tail dependence between each pair of non-ferrous metals is equal to 0, indicating no tail dependence between copper and aluminum, copper and nickel, copper and zinc, or zinc and lead before August 2008.

5.2. The dependence structure between the first and second structural breaks

As shown in Figure 3, the dependence structures between each pair of non-ferrous metals in Period 2 are mostly modeled by sBB1, except for the pair of copper and nickel which is captured by sBB7 copula. Each pair of non-ferrous metals exhibits strong and asymmetrical lower tail dependence, except for the pair of zinc and copper. Zinc is not directly connected with nickel, while nickel has a connection with copper. There are three of four edges connected to zinc in the first tree shown in Figure 3. Thus, the core of metal futures in the dependence

structure becomes zinc in Period 2, which has the strongest impact on the dependence structure between the first and second structural break.

Figure 2: The first tree structure of the R-vine copula in Period 1

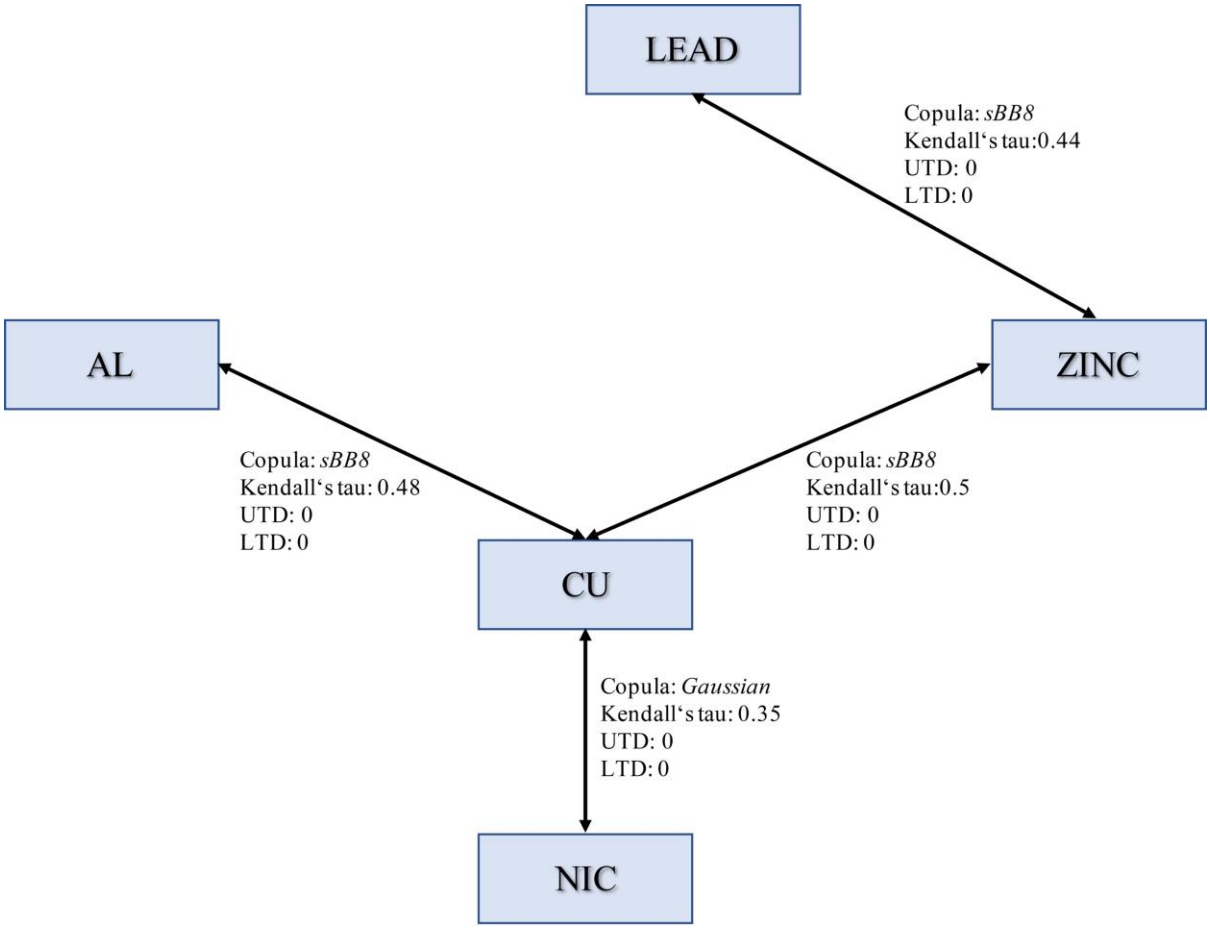

Note: *Copula* denotes the pair-copula family between the corresponding two futures, *Kendall's tau* denotes the value of the pair-copula's Kendall's tau. *UTD* is the value of upper tail dependence coefficient. *LTD* is the value of upper tail dependence coefficient. The core of metal futures is defined to be one of the five non-ferrous metal commodity futures that has the strongest dependence with the remaining four.

Figure 3: The first tree structure of the R-vine copula in Period 2

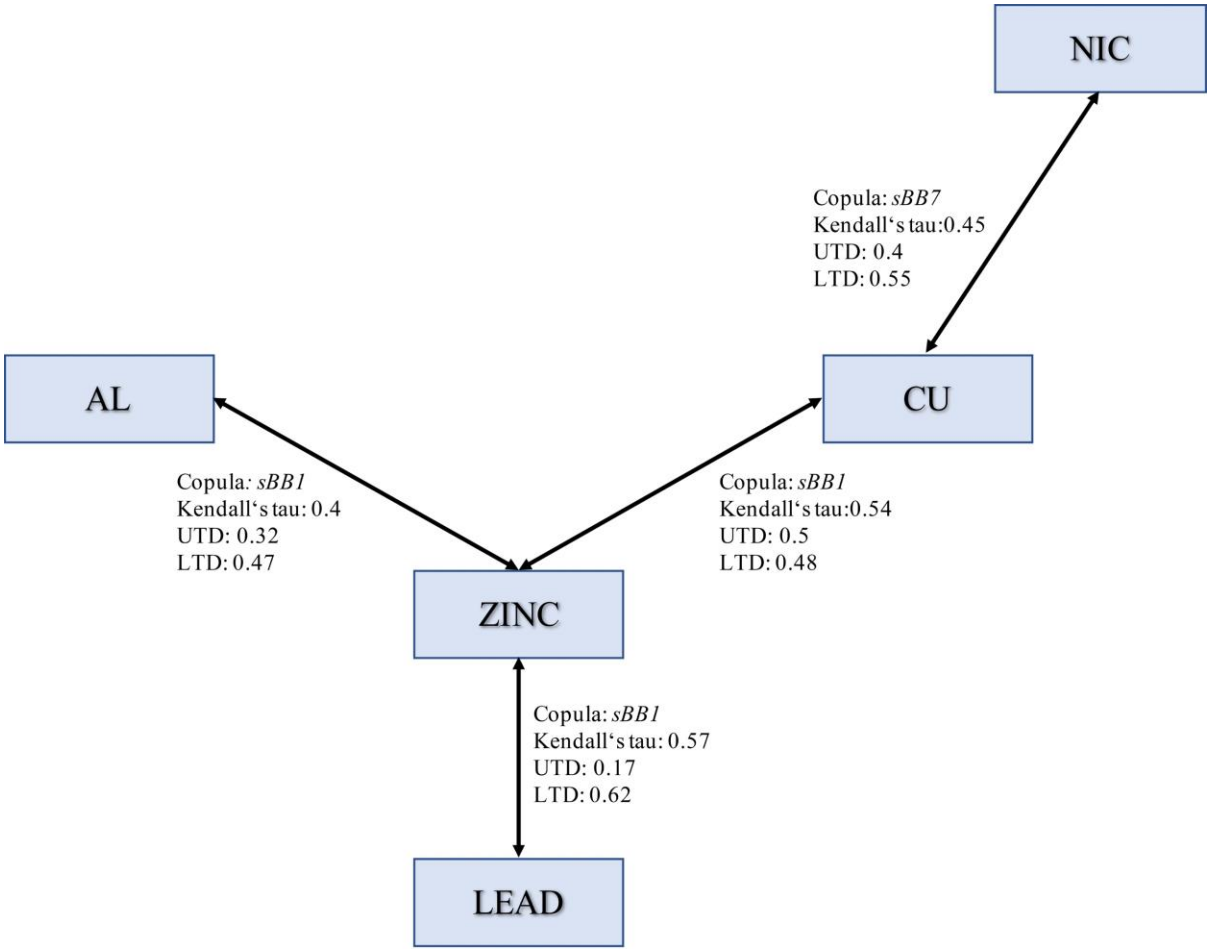

Note: *Copula* denotes the pair-copula family between the corresponding two futures, *Kendall's tau* denotes the value of the pair-copula's Kendall's tau. *UTD* is the value of upper tail dependence coefficient. *LTD* is the value of upper tail dependence coefficient. The core of metal futures is defined to be one of the five non-ferrous metal commodity futures that has the strongest dependence with the remaining four.

5.3. The dependence structure after the second structural break

As shown in Figure 4, there is no tail dependence in most pairs of non-ferrous metals in Period 3, except for the pair of lead and zinc. The Student's *t* copula between lead and zinc indicates symmetrical tail dependence. Similar to Period 1, there are three out of four edges connected to copper in the first tree. Thus, the core of metal futures in the dependence structure

moves back to copper in Period 3, which has the strongest impact on the dependence structure after the second structural break.

Figure 4: The first tree structure of the R-vine copula in Period 3

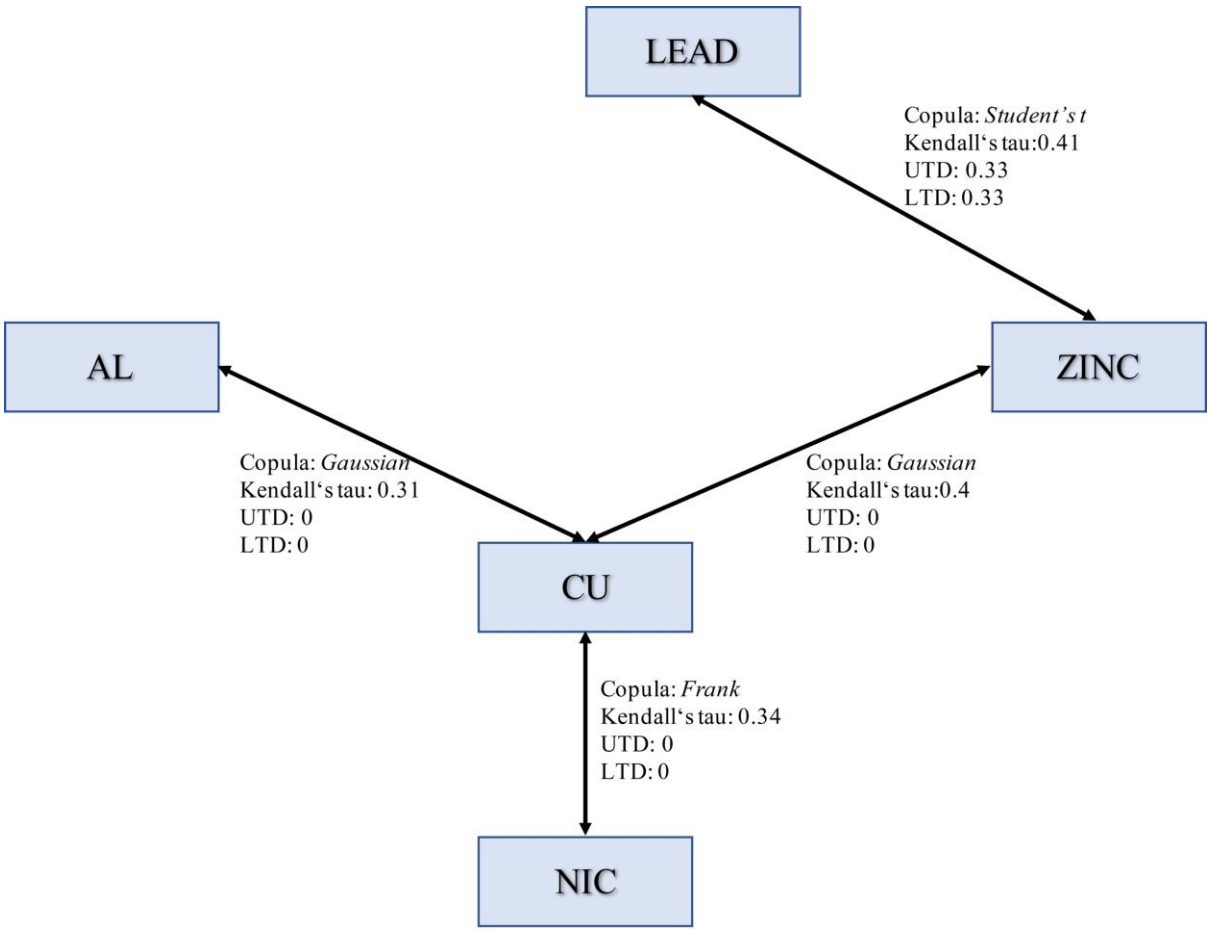

Note: *Copula* denotes the pair-copula family between the corresponding two futures, *Kendall's tau* denotes the value of the pair-copula's Kendall's tau. *UTD* is the value of upper tail dependence coefficient. *LTD* is the value of upper tail dependence coefficient. The core of metal futures is defined to be one of the five non-ferrous metal commodity futures that has the strongest dependence with the remaining four.

5.4. Comparison of dependence structures before and after structural breaks

By analyzing the first-level tree structure formed by the five non-ferrous metal futures before and after the structural breaks, we find that the "general shape" in the first level tree

structure remains unchanged after two structural breaks. In all three periods, the first level tree structure has four edges. Three of them connect directly to the core of non-ferrous metal futures, while the last one combines two non-ferrous metal futures — however, the core metal in the dependence structure changes after the structural breaks. Before the first structural break, copper is in the center of the dependence structure. After the first structural break, zinc take the place of copper and becomes the center of non-ferrous metal futures in the dependence structure. However, after the second structural break, copper moves back to the center of dependence structure between non-ferrous metal futures.

In Table 2, the range of Kendall′s τ in the first tree changes from [0.35, 0.5] to [0.45, 0.57] after the first structural break. The increase in value means that the concordance between the five non-ferrous metal futures becomes stronger, which implies the disappearance of the diversification benefit among the major non-ferrous metal futures. The indices of upper and lower tail dependence in the first tree structure are uniformly equal to 0 before the first structural break. However, the range of the indices of upper and lower tail dependence in the first tree structure drastically increases to [0.17, 0.32] and [0.47,0.62], respectively, after the

first structural break. The overall degree of asymmetrical lower tail dependence between the five non-ferrous metal futures becomes higher after the first structural break.

After the second structural break, the range of Kendall′s τ in the first tree shrinks to [0.31, 0.40], implying a recovery in the diversification benefit among the major non-ferrous metal futures. The indices of upper and lower tail dependence in the first tree structure decrease to 0， except between zinc and lead, which are equal to 0.33. The strong asymmetrical lower tail dependence between the five non-ferrous metal futures disappears after the second structural break.

As shown in Figure 2 and Table 2, before the first structural break, the dependence structure between the five non-ferrous metal futures in the first tree of R-vine is captured by two types of bivariate copulas: Gaussian and sBB8. Note that Gaussian and sBB8 copula cannot measure tail dependence. We conclude that the overall extent of tail dependence is weak before the first structural break. However, after the first structural break, the dependence structure between the five non-ferrous metal futures in the first tree of R-vine is captured by sBB7 and sBB1 copulas. As shown in Figure 3, three of the total four edges are modeled by the sBB1 copulas; the remaining one edge is modeled by sBB7 copula. Note that the sBB1

copula has strong asymmetrical lower tail dependence. Therefore, we confirm the increasing presence of lower tail dependence between the five non-ferrous metal futures in the period between the first and second structural break. After the second structural break, the dependence structure between the five non-ferrous metal futures in the first tree of R-vine is captured by three types of bivariate copulas: Student's *t*, Gaussian and Frank. Among these types of bivariate copula, only Student's *t* has the ability to capture symmetrical tail dependence. Thus, we conclude that the prominent pattern of asymmetrical lower tail dependence between non-ferrous metal futures disappears after the second structural break, while lead and zinc exhibit symmetrical tail dependence.

Table 2. The R-vine copula in Period 1, Period 2 and Period 3

		*Period 1: **Jan, 2002- Aug, 2008***				*Period 2: **Aug, 2008- Jan, 2014***				*Period 3: **Jan, 2014- Dec, 2019***			
Tree1	Margins	**2,3**	**2,1**	**4,2**	**5,4**	**4,1**	**2,3**	**4,2**	**5,4**	**2,3**	**2,1**	**4,2**	**5,4**
	Family	*Gaussian*	*sBB8*	*sBB8*	*sBB8*	*sBB1*	*sBB7*	*sBB1*	*sBB1*	*Frank*	*Gaussian*	*Gaussian*	*Student's t*
	τ	0.35	0.48	0.50	0.44	0.48	0.45	0.54	0.57	0.34	0.31	0.40	0.41
	λ_U	0.00	0.00	0.00	0.00	0.32	0.40	0.50	0.17	0.00	0.00	0.00	0.33
	λ_L	0.00	0.00	0.00	0.00	0.47	0.55	0.48	0.62	0.00	0.00	0.00	0.33
Tree2	Margins	**1,3|2**	**4,1|2**	**5,2|4**		**2,1|4**	**4,3|2**	**5,2|4**		**1,3|2**	**4,1|2**	**5,2|4**	
	Family	*sBB7*	*Gaussian*	*Gaussian*		*Gaussian*	*sGumbel*	*sBB7*		*Gaussian*	*Frank*	*Gaussian*	
	τ	0.16	0.18	0.17		0.21	0.19	0.17		0.16	0.18	0.09	
	λ_U	0.02	0.00	0.00		0.00	0.00	0.02		0.00	0.00	0.00	
	λ_L	0.21	0.00	0.00		0.00	0.24	0.23		0.00	0.00	0.00	
Tree3	Margins	**4,3|1,2**	**5,1|4,2**			**3,1|2,4**	**5,3|4,2**			**4,3|1,2**	**5,1|4,2**		
	Family	*BB7*	*sClayton*			*Gaussian*	*Tawn*			*Clayton*	*Independent*		
	τ	0.08	0.08			0.14	0.09			0.06	0.00		
	λ_U	0.01	0.02			0.00	0.11			0.00	0.00		
	λ_L	0.01	0.00			0.00	0.00			0.01	0.00		
Tree4	Margins	**5,3|4,1,2**				**5,1|3,2,44**				**5,3|4,1,2**			
	Family	*sClayton*				*Independent*				*Independent*			
	τ	0.04				0.00				0.00			
	λ_U	0.00				0.00				0.00			
	λ_L	0.00				0.00				0.00			

Note :1: Aluminum 2: Copper 3: Nickel 4: Zinc 5: Lead, *Student's t*: Student-t copula, *Gaussian*: Gaussian copula, *Frank*: Frank copula, *sClayton*: survival Clayton copula, *sBB1*: survival BB1 copula, *sBB8:*survival BB8 copula, *sBB7:*survival BB7 copula *sGumbel*: survival Gumbel copula, *sClayton*: survival Clayton copula, *Tawn:*Tawn copula, *Independent:* independent copula, τ: Kendall's tau, λ_U: upper tail dependence coefficient, λ_L: lower tail dependence coefficient. θ_1、θ_1 denote the parameters of corresponding copula function. Margins represents a bivariate futures pairs among five metal commodity futures. Family shows bivariate copula fit between margins.

5.4. Discussion of results

It can be observed that copper and zinc dominate the dependence structure across the five non-ferrous metals in different periods. Ciner et al. (2020) examine the return and volatility spillover across non-ferrous metals and report that copper and zinc act as the main stress-transmitters between non-ferrous metals. Literature has also documented a stylized fact, this being that trading volume is positively correlated with volatility in commodity futures markets (see Garcia et al. 1986 and reference therein). In this respect, the relatively large trading volume may bring volatility to the price movement of copper and zinc and can drive information flow from copper and zinc to other non-ferrous metals. Moreover, Wu and Hu (2016) study the sensitivity of volatility clusters to the structural breaks in the non-ferrous metal markets. They suggest that copper and zinc are highly sensitive to structural breaks and that they are overvalued.

As a base industrial material, copper is broadly used in a range of industries such as infrastructure, electronics, automobiles, etc. Consequently, copper has become a barometer of production in the manufacturing and construction industries. Before the crisis, while most developed countries had been suffering from slow economic growth, China's economy was

growing rapidly. The global shift in the manufacturing industry and large-scale urbanization in China created huge demand for copper. From statistics released by the International Copper Study Group (ICSG), the world's copper demand increased from 1.35 million tons in 1998 to 1.81 million tons in 2007 (+34%). Within this 10-year-period, China's copper demand had increased drastically by around 0.35 million tons (+250%), which accounts for almost 80% of the total growth of the world's copper demand[6]. Thus, China had been the driving force of the world's copper demand in the pre-crisis period. Guo (2018) also demonstrates that China's demand for copper significantly affects the international copper market.

As the world's largest producer and consumer of zinc, China accounted for roughly 41.3% of global zinc consumption by 2013[7]. However, there were no zinc futures in China until the Shanghai Futures Exchange (SHFE) launched zinc futures in 2007 to facilitate price discovery in the zinc market and to satisfy zinc companies' increasing demand for risk hedging. Studies on price discovery of the same assets traded in multiple markets reveals that, in spite of the dominant role of the home market, its price discovery process is also significantly affected by

[6] Data source: ICSG 2008 Statistical Yearbook.

[7] Quoted in Aronson, Abel. “Paradigm Shift,” Barron's, May 14, 2011.

foreign markets (Covrig et al., 2009). Literature suggests that information is prone to transmit from larger, more liquid markets to smaller, less liquid markets (e.g. Fung et al., 2003; Schneeweis and Yau, 1990; Xu et al., 2005). Thus, given the dominant role of China in the global zinc market and the late development of Chinese zinc futures, an understanding of SHFE's zinc futures may provide a new perspective that can be used to explain the central role of LME's zinc after the first structural break.

Ciner et al. (2020) document an increase in the level of connectedness between non-ferrous metals during Q3 2007-Q4 2013 and a decrease during Q1 2014-Q4 2016. We find that the level of integration, as well as the degree of lower tail dependence between the five non-ferrous metal futures, was strengthened by the first structural break but weakened by the second structural break. Since the first structural break occurs at August 28, 2008 and the second structural break occurs at January 31, 2014, our findings not only provide solid proof for the aforementioned evidence in Ciner et al. (2020), but also offer accurate and statistically robust dates for the changes. Moreover, the uniform change of integration and tail dependence after two structural breaks can be understood as a common response of the non-ferrous metal futures to the shocks caused by the structural breaks. A natural question to ask is why structural breaks

incur such a response pattern. As mentioned by Gromb and Vayanos (2010) and references cited therein, considerable numbers of investors who have exposures on both equities and commodities are value arbitragers and convergence traders. Once a large shock occurs in stock markets, they are unable to liquidate their risk positions because of borrowing constraints and other pressures. In order to fund the illiquidity, they are more likely to exit the commodity markets at the same time, which forms the commonality in the response pattern of commodity markets and cross-market contagion.

In view of the presence of a common pattern among non-ferrous metals in response to the first structural break triggered by the 2008 financial crisis and the increase in the level of integration across these metals after the crisis, non-ferrous metals, as a whole, are more qualified to be a separate asset class after the crisis. A number of literatures document the evidence of a higher level of integration across multiple markets during or after financial crises. For example, Gerlach et al. (2006) examine the impact of the 1997 Asian financial crisis on the dynamic linkages within several Asia-Pacific real estate markets. They find that the integration level within the Asia-Pacific real estate markets is higher than those suggested by an analysis which incorrectly ignored the crisis. The results in Lu et al. (2012) indicate that the

integration between the US Real Estate Investment Trust (REIT) market and twelve international REIT markets intensifies considerably during turbulent market conditions. Silvennoinena and Thorp (2013) suggest that the integration level across equity, bond and stock markets increases significantly during the crisis period they studied.

6. VaR Forecast and Backtesting Results

In this section, we forecast the out-of-sample VaR of an equal-weighted portfolio and that of individual futures on non-ferrous metals using the scheme described in Section 3.4. The performance of the VaR forecasts are then examined by UC and CC tests, described in Section 3.5[8]. The results of the VaR exceedance test for an equal-weighted portfolio and individual non-ferrous metal futures are shown in Table 3. For comparison, a historical VaR forecast is computed to serve as a benchmark, the results of which are presented in Table 4. The repetition time K, which is defined in section 3.4, is fixed to 5000.

[8] Since the equal-weighted portfolio is widely examined in a number of literatures regarding VaR forecasting (see Siburg et al., 2015; Nikoloulopoulos et al., 2012; Lu et al., 2014). Other types of portfolios, such as the volume-weighted portfolio, can be analyzed in a similar way.

We can see from Table 3 and Table 4 that, in Period 1, almost all UC tests and CC tests for VaR forecasts based on R-vine copula cannot reject the null hypothesis of correct exceedance at 5% significance level, except that of aluminum and zinc. Aluminum rejects the null of α= 1% at 5% significance level and zinc rejects the null of α= 1% and α= 10% at 5% significance level. In contrast, the UC test and CC test for the historical VaR forecast rejects the null hypothesis in most cases. For example, both aforementioned tests for the equal-weighted portfolio reject the null hypothesis of α= 5% and α= 10% at 5% significance level. The UC test for aluminum rejects the null hypothesis of α= 5% at 5% significance level. Nickel rejects the UC and CC tests hypothesizes of α= 1% and α= 10% at 5% significance level. Zinc and lead significantly reject the null hypothesis of both tests at three quantile levels.

The test results in Period 2 are similar to those in Period 1. The UC test and CC test for R-vine copula based VaR forecasts of the equal-weighted portfolio reject the null hypothesis of α= 5% and α= 10% at 5% significance level. The UC test result for copper rejects the null hypothesis of α= 10% at 5% significance level. However, as shown in Table 4, the UC and CC tests for the historical VaR forecast reject the null hypothesis of different quantiles in each case, which creates a sharp contrast with the test results shown in Table 3. In Period 3, only the

UC test for copper's R-vine copula based VaR forecast rejects the null hypothesis of α= 1% at 5% significance level, while the UC and CC tests for the historical VaR forecast cannot reject the null hypothesis of α= 1%, α= 5% and α= 10% in each case.

In a comparative analysis on the results summarized in Table 3 and Table 4, we find that the R-vine copula VaR forecasts show superior forecasting accuracy over the historical VaR forecast in Period 1 and Period 2, regardless of whether in the portfolio case or in the individual futures cases. In Period 3, the R-vine copula VaR forecast performs as well as the benchmark method. These findings lead us to conclude that the R-vine copula VaR forecast has better overall performance than the historical VaR forecasting method.

Table 3(A). VaR exceedance test for Value-at Risk forecast based on R-vine copula

		R-vine copula Value-at-Risk forecast						
		*Period 1**: Jan, 2002- Aug, 2008***			*Period 2: **Aug, 2008- Jan, 2014***		*Period 3: **Jan, 2014- Dec, 2019***	
EW. Port.	**UC test / α**	**1%**	**5%**	**10%**	**5%**	**10%**	**5%**	**10%**
	Exp.exceed	1	6	13	5	11	6	12
	Act. Exceed	1	11	16	2	4	3	8
	p-value	0.7324	0.1389	0.5416	0.0678	0.0084	0.1444	0.1616
	Decision	*Not Rej.*	*Not Rej.*	*Not Rej.*	*Not Rej.*	*Rej.*	*Not Rej.*	*Not Rej.*
	CC test / α	**1%**	**5%**	**10%**	**5%**	**10%**	**5%**	**10%**
	p-value	0.9363	0.1279	0.6153	0.1820	0.0268	0.3197	0.2151
	Decision	*Not Rej.*	*Not Rej.*	*Not Rej.*	*Not Rej.*	*Rej.*	*Not Rej.*	*Not Rej.*
AL	**UC test / α**	**1%**	**5%**	**10%**	**5%**	**10%**	**5%**	**10%**
	Exp.exceed	1	6	13	5	11	6	12
	Act. Exceed	6	8	13	3	6	4	13
	p-value	0.0034	0.6749	0.8189	0.2037	0.0661	0.3336	0.8585
	Decision	*Rej.*	*Not Rej.*	*Not Rej.*	*Not Rej.*	*Not Rej.*	*Not Rej.*	*Not Rej.*
	CC test / α	**1%**	**5%**	**10%**	**5%**	**10%**	**5%**	**10%**
	p-value	0.0105	0.5574	0.7559	0.4108	0.1320	0.5478	0.2110
	Decision	*Rej.*	*Not Rej.*	*Not Rej.*	*Not Rej.*	*Not Rej.*	*Not Rej.*	*Not Rej.*

Table 3(B). VaR exceedance test for Value-at Risk forecast based on R-vine copula

		R-vine copula Value-at-Risk forecast						
		*Period 1**: Jan, 2002- Aug, 2008***			*Period 2: **Aug, 2008- Jan, 2014***		*Period 3: **Jan, 2014- Dec, 2019***	
CU	**UC test / α**	**1%**	**5%**	**10%**	**5%**	**10%**	**5%**	**10%**
	Exp.exceed	1	6	13	5	11	6	12
	Act. Exceed	2	11	16	2	5	2	8
	p-value	0.6191	0.1389	0.5416	0.0678	0.0261	0.0449	0.1616
	Decision	*Not Rej.*	*Not Rej.*	*Not Rej.*	*Not Rej.*	*Rej.*	*Rej.*	*Not Rej.*
	CC test / α	**1%**	**5%**	**10%**	**5%**	**10%**	**5%**	**10%**
	p-value	0.8580	0.1401	0.6567	0.1820	0.0668	0.1295	0.2151
	Decision	*Not Rej.*	*Not Rej.*	*Not Rej.*	*Not Rej.*	*Not Rej.*	*Not Rej.*	*Not Rej.*
NIC	**UC test / α**	**1%**	**5%**	**10%**	**5%**	**10%**	**5%**	**10%**
	Exp.exceed	1	6	13	5	11	6	12
	Act. Exceed	1	8	18	2	7	3	9
	p-value	0.7324	0.6749	0.2526	0.0678	0.1418	0.1444	0.2869
	Decision	*Not Rej.*	*Not Rej.*	*Not Rej.*	*Not Rej.*	*Not Rej.*	*Not Rej.*	*Not Rej.*
	CC test / α	**1%**	**5%**	**10%**	**5%**	**10%**	**5%**	**10%**
	p-value	0.9363	0.5574	0.4999	0.1820	0.2140	0.3197	0.2785
	Decision	*Not Rej.*	*Not Rej.*	*Not Rej.*	*Not Rej.*	*Not Rej.*	*Not Rej.*	*Not Rej.*

Table 3(C). VaR exceedance test for Value-at Risk forecast based on R-vine copula

		R-vine copula Value-at-Risk forecast						
		*Period 1**: Jan, 2002- Aug, 2008***			*Period 2: **Aug, 2008- Jan, 2014***		*Period 3: **Jan, 2014- Dec, 2019***	
ZINC	**UC test / α**	**1%**	**5%**	**10%**	**5%**	**10%**	**5%**	**10%**
	Exp.exceed	1	6	13	5	11	6	12
	Act. Exceed	5	15	19	2	6	7	14
	p-value	0.0167	0.0058	0.1602	0.0678	0.0661	0.7465	0.6382
	Decision	*Rej.*	*Rej.*	*Not Rej.*	*Not Rej.*	*Not Rej.*	*Not Rej.*	*Not Rej.*
	CC test / α	**1%**	**5%**	**10%**	**5%**	**10%**	**5%**	**10%**
	p-value	0.0471	0.0213	0.3480	0.1820	0.1320	0.6510	0.7650
	Decision	*Rej.*	*Rej.*	*Not Rej.*	*Not Rej.*	*Not Rej.*	*Not Rej.*	*Not Rej.*
LEAD	**UC test / α**	**1%**	**5%**	**10%**	**5%**	**10%**	**5%**	**10%**
	Exp.exceed	1	6	13	5	11	6	12
	Act. Exceed	3	9	17	3	6	3	8
	p-value	0.2304	0.4324	0.3791	0.2037	0.0661	0.1444	0.1616
	Decision	*Not Rej.*	*Not Rej.*	*Not Rej.*	*Not Rej.*	*Not Rej.*	*Not Rej.*	*Not Rej.*
	CC test / α	**1%**	**5%**	**10%**	**5%**	**10%**	**5%**	**10%**
	p-value	0.4555	0.3900	0.6767	0.4108	0.1320	0.3197	0.2151
	Decision	*Not Rej.*	*Not Rej.*	*Not Rej.*	*Not Rej.*	*Not Rej.*	*Not Rej.*	*Not Rej.*

Note: **AL**: Aluminum **CU:** Copper **NIC:** Nickel. **EW. Port.:** equally weighted portfolio. In each forecast step, the number of simulated observations for each metal commodity future is fixed to K=5000. ***R-vine copula Value-at-Risk forecast*** shows the results of VaR exceedance test for VaR generated by the scheme described in Section 3.4. Exp.exceed denotes the expected number of exceedances, Act.exceed denotes the actual number of exceedances, Decision represents the final decision of the corresponding statistical test at 5% significance level. Stat. denotes the value of corresponding test statistic. α is the percentile threshold of VaR. In most cases during *Period 2*, no actual violation creates a zero denominator which leads to the invalidation of the unconditional coverage test, therefore, the test results of q=1% are not shown in this table.

Table 4(A). VaR exceedance test for historical Value-at Risk forecast

		Historical Value-at-Risk forecast						
		*Period 1**: Jan, 2002- Aug, 2008***			*Period 2: **Aug, 2008- Jan, 2014***		*Period 3: **Jan, 2014- Dec, 2019***	
EW. Port.	**UC test / α**	**1%**	**5%**	**10%**	**5%**	**10%**	**5%**	**10%**
	Exp.exceed	1	6	13	5	11	6	12
	Act. Exceed	4	14	27	2	4	7	11
	p-value	0.0683	0.0143	0.0008	0.0678	0.0084	0.7465	0.6698
	Decision	*Not Rej.*	*Rej.*	*Rej.*	*Not Rej.*	*Rej.*	*Not Rej.*	*Not Rej.*
	CC test / α	**1%**	**5%**	**10%**	**5%**	**10%**	**5%**	**10%**
	p-value	0.1682	0.0455	0.0035	0.1820	0.0268	0.6219	0.9129
	Decision	*Not Rej.*	*Rej.*	*Rej.*	*Not Rej.*	*Rej.*	*Not Rej.*	*Not Rej.*
AL	**UC test / α**	**1%**	**5%**	**10%**	**5%**	**10%**	**5%**	**10%**
	Exp.exceed	1	6	13	5	11	6	12
	Act. Exceed	4	13	21	2	4	8	14
	p-value	0.0683	0.0328	0.0557	0.0678	0.0084	0.4769	0.6382
	Decision	*Not Rej.*	*Rej.*	*Not Rej.*	*Not Rej.*	*Rej.*	*Not Rej.*	*Not Rej.*
	CC test / α	**1%**	**5%**	**10%**	**5%**	**10%**	**5%**	**10%**
	p-value	0.1682	0.0795	0.1415	0.1820	0.0268	0.4449	0.1475
	Decision	*Not Rej.*	*Not Rej.*	*Not Rej.*	*Not Rej.*	*Rej.*	*Not Rej.*	*Not Rej.*

Table 4(B). VaR exceedance test for historical Value-at Risk forecast

		Historical Value-at-Risk forecast						
		*Period 1**: Jan, 2002- Aug, 2008***			*Period 2: **Aug, 2008- Jan, 2014***		*Period 3: **Jan, 2014- Dec, 2019***	
CU	**UC test / α**	**1%**	**5%**	**10%**	**5%**	**10%**	**5%**	**10%**
	Exp.exceed	1	6	13	5	11	6	12
	Act. Exceed	4	10	20	1	5	5	9
	p-value	0.0683	0.2551	0.0968	0.0134	0.0261	0.6094	0.2869
	Decision	*Not Rej.*	*Not Rej.*	*Not Rej.*	*Rej.*	*Rej.*	*Not Rej.*	*Not Rej.*
	CC test / α	**1%**	**5%**	**10%**	**5%**	**10%**	**5%**	**10%**
	p-value	0.1682	0.4777	0.2488	0.0465	0.0668	0.7100	0.2785
	Decision	*Not Rej.*	*Not Rej.*	*Not Rej.*	*Rej.*	*Not Rej.*	*Not Rej.*	*Not Rej.*
NIC	**UC test / α**	**1%**	**5%**	**10%**	**5%**	**10%**	**5%**	**10%**
	Exp.exceed	1	6	13	5	11	6	12
	Act. Exceed	5	12	23	1	7	6	10
	p-value	0.0167	0.0700	0.0161	0.0134	0.1418	0.9340	0.4587
	Decision	*Rej.*	*Not Rej.*	*Rej.*	*Rej.*	*Not Rej.*	*Not Rej.*	*Not Rej.*
	CC test / α	**1%**	**5%**	**10%**	**5%**	**10%**	**5%**	**10%**
	p-value	0.0471	0.1935	0.0263	0.0465	0.2140	0.7325	0.3133
	Decision	*Rej.*	*Not Rej.*	*Rej.*	*Rej.*	*Not Rej.*	*Not Rej.*	*Not Rej.*

Table 4(C). VaR exceedance test for historical Value-at Risk forecast of individual non-ferrous metal futures

		Historical Value-at-Risk forecast						
		*Period 1**: Jan, 2002- Aug, 2008***			*Period 2: **Aug, 2008- Jan, 2014***		*Period 3: **Jan, 2014- Dec, 2019***	
ZINC	**UC test / α**	**1%**	**5%**	**10%**	**5%**	**10%**	**5%**	**10%**
	Exp.exceed	1	6	13	5	11	6	12
	Act. Exceed	6	20	30	0	5	8	18
	p-value	0.0034	0.0000	0.0000	-	0.0261	0.4769	0.1137
	Decision	*Rej.*	*Rej.*	*Rej.*	-	*Rej.*	*Not Rej.*	*Not Rej.*
	CC test / α	**1%**	**5%**	**10%**	**5%**	**10%**	**5%**	**10%**
	p-value	0.0105	0.0001	0.0003	-	0.0668	0.6319	0.2560
	Decision	*Rej.*	*Rej.*	*Rej.*	-	*Not Rej.*	*Not Rej.*	*Not Rej.*
LEAD	**UC test / α**	**1%**	**5%**	**10%**	**5%**	**10%**	**5%**	**10%**
	Exp.exceed	1	6	13	5	11	6	12
	Act. Exceed	8	16	31	0	3	7	12
	p-value	0.0000	0.0022	0.0000	-	0.0021	0.7465	0.9042
	Decision	*Rej.*	*Rej.*	*Rej.*	-	*Rej.*	*Not Rej.*	*Not Rej.*
	CC test / α	**1%**	**5%**	**10%**	**5%**	**10%**	**5%**	**10%**
	p-value	0.0003	0.0011	0.0000	-	0.0081	0.6219	0.2706
	Decision	*Rej.*	*Rej.*	*Rej.*	-	*Rej.*	*Not Rej.*	*Not Rej.*

Note: **AL**: Aluminum **CU:** Copper **NIC:** Nickel. **EW. Port.:** equally weighted portfolio. In each forecast step, the number of simulated observations for each metal commodity future is fixed to K=5000. ***Historical Value-at-Risk forecast*** denotes the results of VaR exceedance test for historical VaR. Exp.exceed denotes the expected number of exceedances, Act.exceed denotes the actual number of exceedances, Decision represents the final decision of the corresponding statistical test at 5% significance level. Stat. denotes the value of corresponding test statistic. α is the percentile threshold of VaR. In most cases during *Period 2*, no actual violation creates a zero denominator which leads to the invalidation of the unconditional coverage test, therefore, the test results of q=1% are not shown in this table.

The VaR forecast and corresponding realized returns of the equal-weighted portfolio and each non-ferrous metal futures are shown in Figure 5 - Figure 7. The blue line denotes the time series of the realized returns and the red dotted line denotes the time series of the VaR forecast at $\alpha = 1\%$. The brown dotted line denotes the time series of the VaR forecast at $\alpha = 5\%$ and the yellow dotted line denotes the time series of the VaR forecast at $\alpha = 10\%$. In Period 1, we observe that the realized returns of the equal-weighted portfolio and each individual non-ferrous metal futures exceed the VaR forecast at $\alpha = 1\%$ at least once. However, as shown in Figure 6 and Figure 7, the realized returns of the equal-weighted portfolio and each non-ferrous metal futures do not exceed the associated VaR forecast at $\alpha = 1\%$ in Period 2 and Period 3. These evidences firmly support the findings and results in Table 3 and Table 4.

Figure 5: Realized returns and VaR forecast for equally weighted portfolio and individual non-ferrous metal futures in Period 1

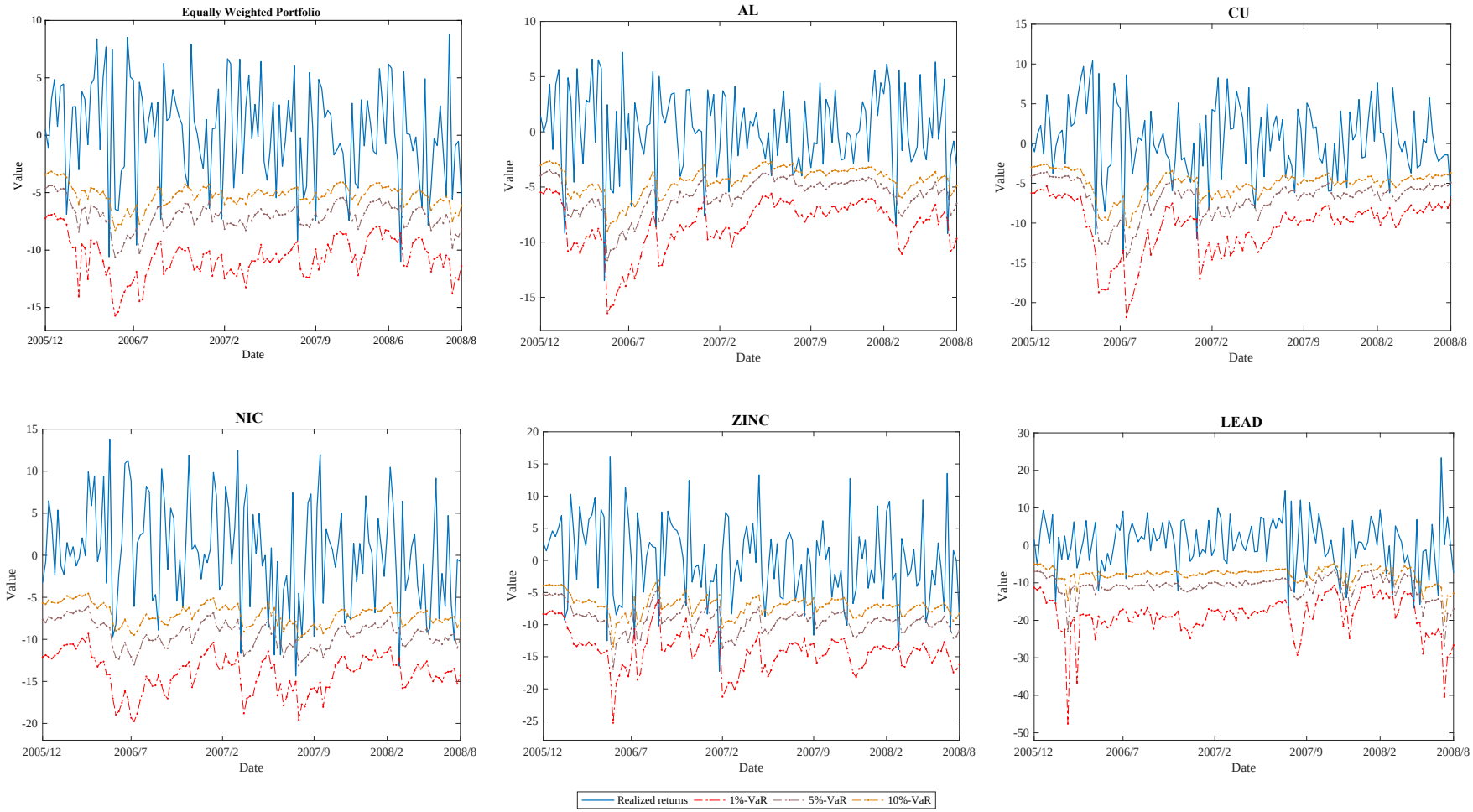

Note: Realized Returns denotes non-ferrous metal futures returns. *q*%-VaR is the *q*-percentile VaR for individual futures.

Figure 6: Realized returns and VaR forecast for equally weighted portfolio and individual non-ferrous metal futures in Period 2

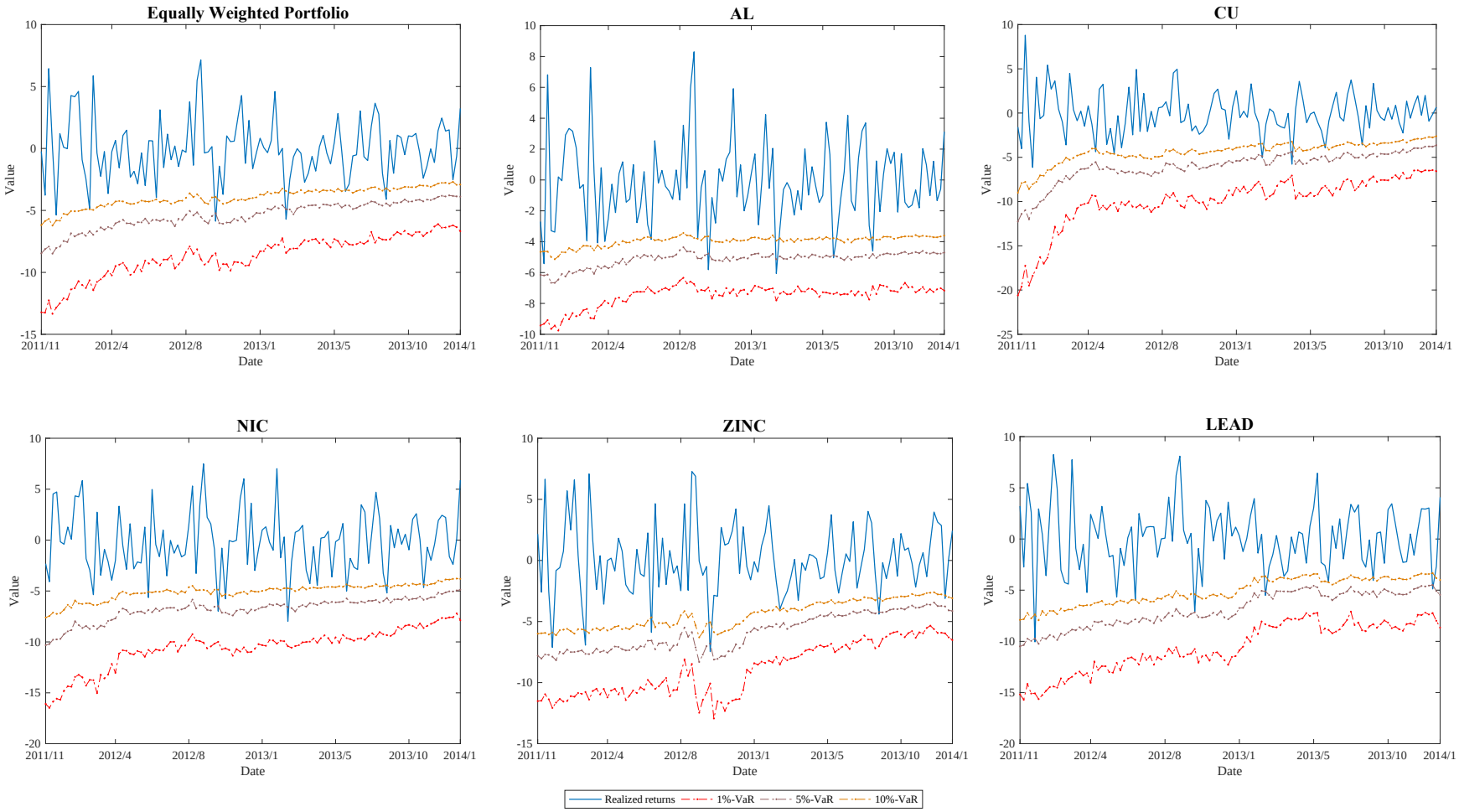

Note: Realized Returns denotes non-ferrous metal futures returns. *q*%-VaR is the *q*-percentile VaR for individual futures.

Figure 7: Realized returns and VaR forecast for equally weighted portfolio and individual non-ferrous metal futures in Period 3

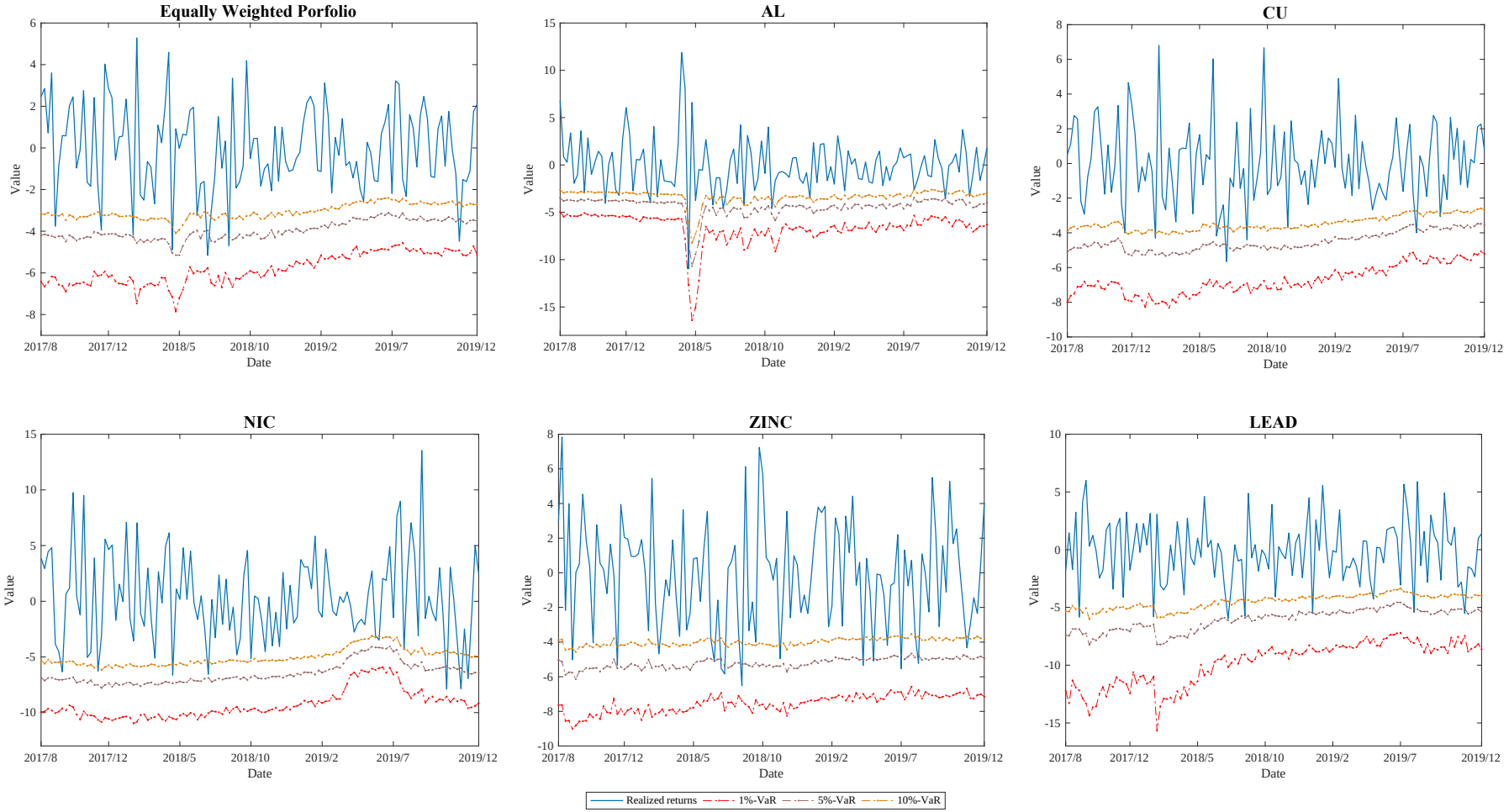

Note: Realized Returns denotes non-ferrous metal futures returns. *q*%-VaR is the *q*-percentile VaR for individual futures.

7. Conclusion

In this paper, we employ an R-vine copula to investigate the dependence structure of non-ferrous metal commodity futures in three periods which are determined by two structural breaks. Our empirical results from the R-vine copula generate valuable insights for market participants, investors and speculators. Firstly, we find that the center of the dependence structure between the five non-ferrous metal futures changes from copper to zinc after the first structural break in 2008 and moves back to copper after the second structural break in 2014. During the period between 2008 and 2014, we argue that non-ferrous metals, as a whole, are more suited to be regarded as a separate asset class, which is consistent with Ciner et al. (2020). This is due to our observations that the risk diversification benefit among them diminishes and there is a significant increase in tail dependence between them. However, the presence of a high level of integration and strong lower tail dependence between non-ferrous metals has perished after the second structural break. The R-vine copula-based method shows superior performance for both the equal-weighted portfolio and individual futures in the out-of-sample data. The VaR forecast scheme we developed in this paper can be used as a useful tool for institutional investors (e.g., index-tracking ETF managers, CTAs) to manage the risk of their

portfolio or individual commodities. Future research may focus on investigating the impact of COVID-19 on the dependence structure of non-ferrous metals.

Acknowledgement

We would like to thank two anonymous referees for their constructive comments, which helps to improve the quality of this paper. We are also grateful for the comments from Professor Joe Byers from Oklahoma State University and Nikola Vasiljević from University of Zurich. The responsibility of any error in the paper remains ours. Versions of the paper have been presented at European Financial Management Association (EFMA) 2019 annual meeting, Forecasting Financial Markets (FFM) 2019 annual meeting, China International Risk Forum & China Finance Review International 2020 Joint Conference and Renmin University of China.

References

Aas, Kjersti, Claudia Czado, Arnoldo Frigessi, and Henrik Bakken. 2009. “Pair-Copula Constructions of Multiple Dependence.” *Insurance: Mathematics and Economics* 44 (2): 182–198.

Abbara, Omar, and Mauricio Zevallos. 2014. “Assessing Stock Market Dependence AndContagion.” *Quantitative Finance* 14(9):1627–1641.

Aggarwal, Raj, Brian Lucey, and Fergal Oconnor. 2015. “World Metal Markets.” *The World Scientific Handbook of Futures Markets World Scientific Handbook in Financial Economics Series*, 325–347.

Apergis, Nicholas, Giray Gozgor, Chi Keung Marco Lau, and Shixuan Wang. 2020 “Dependence structure in the Australian electricity markets: New evidence from regular vine copulae.” *Energy Economics* 90 (2020): 104834.

Bedford, Tim, and Roger M. Cooke. 2002. “Vines--a New Graphical Model for Dependent Random Variables.” *The Annals of Statistics* 30 (4): 1031–1068.

Bollerslev, Tim. 1987. “A Conditionally Heteroskedastic Time Series Model for Speculative Prices and Rates of Return.” *The Review of Economics and Statistics* 69 (3): 542.

Box, George and Jenkins, Gwilym. 1976. “Time Series Analysis: Forecasting and Control”. *Holden-Day*.

Brechmann, Eike Christain, and Claudia Czado. 2013. “Risk Management with High-Dimensional Vine Copulas: An Analysis of the Euro Stoxx 50.” *Statistics & Risk Modeling* 30 (4).

Bücher, Axel, and Ivan Kojadinovic. 2016. “A Dependent Multiplier Bootstrap for the Sequential Empirical Copula Process under Strong Mixing.” *Bernoulli*22 (2): 927–68.

Brio, Esther B. Del, Andrés Mora-Valencia, and Javier Perote. 2018. “Risk Quantification for Commodity ETFs: Backtesting Value-at-Risk and Expected Shortfall.” *International Review of Financial Analysis* (forthcoming).

Choi, Kyongwook, and Shawkat Hammoudeh. 2010. “Volatility Behavior of Oil, Industrial Commodity and Stock Markets in a Regime-Switching Environment.” *Energy Policy* 38 (8): 4388–4399.

Christoffersen, P. 2004. “Backtesting Value-at-Risk: A Duration-Based Approach.” *Journal of Financial Econometrics* 2 (1): 84–108.

Christoffersen, Peter F. 1998. “Evaluating Interval Forecasts.” *International Economic*

Review 39 (4): 841.

Ciner, Cetin. 2001. “On the Long Run Relationship between Gold and Silver Prices A Note.” *Global Finance Journal* 12 (2): 299–303.

Ciner, Cetin, Brian Lucey, and Larisa Yarovaya. 2020. “Spillovers, Integration and Causality in LME Non-Ferrous Metal Markets.” *Journal of Commodity Markets* 17: 100079.

Covrig, Vicentiu, David K. Ding, and Buen Sin Low. 2004. “The Contribution of a Satellite Market to Price Discovery: Evidence from the Singapore Exchange.” *Journal of Futures Markets* 24 (10): 981–1004.

Chang, Eric C., and Chan-Wung Kim. 1988. “Day of the Week Effects and Commodity Price Changes.” *Journal of Futures Markets* 8 (2): 229–41.

Chen, Honghui, and Vijay Singal. 2003. “Role of Speculative Short Sales in Price Formation: The Case of the Weekend Effect.” *The Journal of Finance* 58 (2): 685–705.

Dulaney, Tim, Tim Husson, and Craig J. McCann. 2012 "Leveraged, Inverse, and Futures-Based Etfs." *PIABA Bar Journal* 19 (1): 83-107

Dißmann, J., E.c. Brechmann, C. Czado, and D. Kurowicka. 2013. “Selecting and Estimating Regular Vine Copulae and Application to Financial Returns.” *Computational Statistics & Data Analysis* 59: 52–69.

Embrechts, Paul, Alexander J. Mcneil, and Daniel Straumann. 2002. “Correlation and Dependence in Risk Management: Properties and Pitfalls.” *Risk Management*, October, 176–223.

Engle, Robert F., and Victor K. Ng. 1993. “Measuring and Testing the Impact of News on Volatility.” *The Journal of Finance* 48 (5): 1749–78.

Engle, Robert F. 1982. “Autoregressive Conditional Heteroscedasticity with Estimates of the Variance of United Kingdom Inflation.” *Econometrica* 50 (4): 987.

Francq, Christian, and Zakoïan Jean-Michel. 2019. *GARCH Models: Structure, Statistical Inference and Financial Applications*. Hoboken, NJ: John Wiley & Sons.

Fischer, Matthias, Christian Köck, Stephan Schlüter, and Florian Weigert. 2009. “An Empirical Analysis of Multivariate Copula Models.” *Quantitative Finance* 9 (7): 839–854.

Fung, Hung-Gay, Wai K. Leung, and Xiaoqing Eleanor Xu. 2003. "Information flows between the US and China commodity futures trading." *Review of Quantitative Finance and Accounting* 21 (3): 267-285.

Guedj, Ilan, Guohua Li, and Craig Mccann. 2011. “Futures-Based Commodity ETFs.” *The Journal of Index Investing* 2 (1): 14–24.

Glosten, Lawrence R., Ravi Jagannathan, and David E. Runkle. 1993. “On the Relation between the Expected Value and the Volatility of the Nominal Excess Return on Stocks.” *The Journal of Finance* 48 (5): 1779–1801.

Gerlach, Richard, Patrick Wilson, and Ralf Zurbruegg. 2006. “Structural Breaks and Diversification: The Impact of the 1997 Asian Financial Crisis on the Integration of Asia-Pacific Real Estate Markets.” *Journal of International Money and Finance* 25 (6): 974–991.

Gay, Gerald D., and Tae-Hyuk Kim. 1987. “An Investigation into Seasonality in the Futures Market.” *Journal of Futures Markets*7 (2): 169–81.

Garcia, Philip, Raymond M. Leuthold, and Hector Zapata. 1986. “Lead-lag relationships between trading volume and price variability: New evidence.” *The Journal of Futures Markets (1986-1998)* 6(1): 1.

Haff, Ingrid Hobæk, Kjersti Aas, and Arnoldo Frigessi. 2010. “On the Simplified Pair-Copula Construction — Simply Useful or Too Simplistic?” *Journal of Multivariate Analysis*101 (5): 1296–1310.

Hillier, David, Paul Draper, and Robert Faff. 2006. “Do Precious Metals Shine? An Investment Perspective.” *Financial Analysts Journal* 62 (2): 98–106.

Hunter, William Curt, George G. Kaufman, and Michael Pomerleano, eds. 2003. *Asset price bubbles: Implications for monetary, regulatory, and international Policies*. MA: MIT Press.

Huang, Wanling and Ning, Cathy. 2017. “Is the inter- and intra- continental diversification potential disappearing? A vine copula approach”, PhD diss., University of Texas Rio Grande Valley.

Hill, Joanne, Thomas Schneeweis, and Jot Yau. 1990. “International Trading/Nontrading Time Effects on Risk Estimation in Futures Markets.” *Journal of Futures Markets* 10 (4): 407–23.

Inclan, Carla, and George C. Tiao. 1994. “Use of Cumulative Sums of Squares for Retrospective Detection of Changes of Variance.” *Journal of the American Statistical Association* 89 (427): 913.

Jensen, Gerald R., Robert R. Johnson, and Jeffrey M. Mercer. 2002. “Tactical Asset Allocation and Commodity Futures.” *The Journal of Portfolio Management* 28 (4):

100–111.

Joe, Harry, Haijun Li, and Aristidis K. Nikoloulopoulos. 2010. “Tail Dependence Functions and Vine Copulas.” *Journal of Multivariate Analysis* 101 (1): 252–270.

Junker, Markus, and Angelika May. 2005. “Measurement of Aggregate Risk with Copulas.” *The Econometrics Journal* 8 (3): 428–454.

Killiches, Matthias, Daniel Kraus, and Claudia Czado. 2017. “Examination and Visualisation of the Simplifying Assumption for Vine Copulas in Three Dimensions.” *Australian & New Zealand Journal of Statistics* 59 (1): 95–117.

Kojadinovic, Ivan, Jean-François Quessy, and Tom Rohmer. 2015. “Testing the Constancy of Spearman’s Rho in Multivariate Time Series.” *Annals of the Institute of Statistical Mathematics*68 (5): 929–54.

Liew, Rong Qi, and Yuan Wu. 2013. “Pairs Trading: A Copula Approach.” *Journal of Derivatives & Hedge Funds* 19 (1): 12–30.

Longin, François, and Bruno Solnik. 2001. “Extreme Correlation of International Equity Markets.” *The Journal of Finance* 56 (2): 649–676.

Low, Rand Kwong Yew, Jamie Alcock, Robert Faff, and Timothy Brailsford. 2013. “Canonical Vine Copulas in the Context of Modern Portfolio Management: Are They Worth It?” *Journal of Banking & Finance* 37 (8): 3085–3099.

Lu, Xun Fa, Kin Keung Lai, and Liang Liang. 2011. “Portfolio Value-at-Risk Estimation in Energy Futures Markets with Time-Varying Copula-GARCH Model.” *Annals of Operations Research* 219 (1): 333–357.

Lyócsa, Štefan, Peter Molnár, and Neda Todorova. 2017. “Volatility Forecasting of Non-Ferrous Metal Futures: Covariances, Covariates or Combinations?” *Journal of International Financial Markets, Institutions and Money* 51: 228–247.

Li, Xiafei, and Yu Wei. 2018. “The Dependence and Risk Spillover between Crude Oil Market and China Stock Market: New Evidence from a Variational Mode Decomposition-Based Copula Method.” *Energy Economics* 74: 565–81.

Lu, Chiuling, Yiuman Tse, and Michael Williams. 2012. “Returns Transmission, Value at Risk, and Diversification Benefits in International REITs: Evidence from the Financial Crisis.” *Review of Quantitative Finance and Accounting* 40 (2): 293–318.

Mensi, Walid, Aviral Tiwari, Elie Bouri, David Roubaud, and Khamis H. Al-Yahyaee. 2017. “The Dependence Structure across Oil, Wheat, and Corn: A Wavelet-Based Copula Approach Using Implied Volatility Indexes.” *Energy Economics* 66: 122–39.

Mcneil, Alexander J., and Johanna Nešlehová. 2009. “Multivariate Archimedean Copulas, d-Monotone Functions and ℓ1-Norm Symmetric Distributions.” The Annals of Statistics 37 (5B): 3059–3097.

Markwat, Thijs. 2014. “The Rise of Global Stock Market Crash Probabilities.” *Quantitative Finance* 14 (4): 557–571.

Malte S. Kurz and Fabian Spanhel. 2017. “Testing the simplifying assumption in high-dimensional vine copulas.” *ArXiv e-prints.* https://arxiv.org/abs/1706.02338.

Morales Napoles, Oswaldo, Roger M. Cooke, and Dorota Kurowicka. 2010. “About the number of vines and regular vines on n nodes”. PhD diss., Technische Universiteit Delft.

Manner, Hans. 2007. *Estimation and Model Selection of Copulas with an Application to Exchange Rates.* Maastricht: METEOR, Maastricht research school of Economics of TEchnology and ORganizations.

Malte S. Kurz. 2019. “pacotest: Testing for Partial Copulas and the Simplifying Assumption in Vine Copulas”. *R package version 0.3.1*.

Nagler, Thomas, Schepsmeier, Ulf, Stoeber, Jakob, Eike Christian, Brechmann, Graeler, Benedikt, Erhardt, Tobias, Almeida, Carlos et al. 2019. “VineCopula: Statistical Inference of Vine Copulas.” *R package version 2.3.0.* https://CRAN.R-project.org/package=VineCopula

Nelsen, Roger B. 2011. *An Introduction to Copulas*. New York: Springer.

Nagler, Thomas, and Claudia Czado. 2016. “Evading the Curse of Dimensionality in Nonparametric Density Estimation with Simplified Vine Copulas.” *Journal of Multivariate Analysis* 151: 69–89.

Nikoloulopoulos, Aristidis K., Harry Joe, and Haijun Li. 2012. “Vine Copulas with Asymmetric Tail Dependence and Applications to Financial Return Data.” *Computational Statistics & Data Analysis* 56 (11): 3659–3673.

Ning, Cathy. 2010. “Dependence Structure between the Equity Market and the Foreign Exchange Market–A Copula Approach.” *Journal of International Money and Finance* 29 (5): 743–759.

Patton, A. J. 2004. “On the Out-of-Sample Importance of Skewness and Asymmetric Dependence for Asset Allocation.” *Journal of Financial Econometrics* 2 (1): 130–168.

Patton, Andrew J. 2006. “Modelling Asymmetric Exchange Rate Dependence*.” *International Economic Review* 47 (2): 527–556.

Pircalabu, Anca, and Jesper Jung. 2017. “A Mixed C-Vine Copula Model for Hedging Price and Volumetric Risk in Wind Power Trading.” *Quantitative Finance* 17 (10): 1583–1600.

Scherer, Bernd, and Li He. 2011. “The Diversification Benefits of Commodity Futures Indexes: A Mean-Variance Spanning Test.” In *The Handbook of Commodity Investing*, 241–65.

Sensoy, Ahmet. 2013. “Dynamic Relationship between Precious Metals.” *Resources Policy* 38 (4): 504–511.

Siburg, Karl Friedrich, Pavel Stoimenov, and Gregor N.f. Weiß. 2015. “Forecasting Portfolio-Value-at-Risk with Nonparametric Lower Tail Dependence Estimates.” *Journal of Banking & Finance* 54: 129–140.

So, Mike K.p., and Cherry Y.t. Yeung. 2014. “Vine-Copula GARCH Model with Dynamic Conditional Dependence.” *Computational Statistics & Data Analysis* 76: 655–671.

Silvennoinen, Annastiina, and Susan Thorp. 2013. “Financialization, Crisis and Commodity Correlation Dynamics.” *Journal of International Financial Markets, Institutions and Money* 24: 42–65.

Singal, Vijay, and Jitendra Tayal. 2019. “Risky Short Positions and Investor Sentiment: Evidence from the Weekend Effect in Futures Markets.” *Journal of Futures Markets*40 (3): 479–500.

Todorova, Neda, and Adam E. Clements. 2018. “The Volatility-Volume Relationship in the LME Futures Market for Industrial Metals.” *Resources Policy* 58: 111–24.

Tiwari, Aviral Kumar, Goodness C. Aye, Rangan Gupta, and Konstantinos Gkillas. 2020. “Gold-Oil Dependence Dynamics and the Role of Geopolitical Risks: Evidence from a Markov-Switching Time-Varying Copula Model.” *Energy Economics* 88: 104748.

Vigne, Samuel A., Brian M. Lucey, Fergal A. O’Connor, and Larisa Yarovaya. 2017. “The Financial Economics of White Precious Metals — A Survey.” *International Review of Financial Analysis* 52: 292–308.

Watkins, Clinton, and Michael Mcaleer. 2004. “Econometric Modelling of Non-Ferrous Metal Prices.” *Journal of Economic Surveys* 18 (5): 651–701.

Watkins, Clinton, and Michael Mcaleer. 2006. “Pricing of Non-Ferrous Metals Futures on the London Metal Exchange.” *Applied Financial Economics* 16 (12): 853–880.

Weiß, Gregor N.f., and Hendrik Supper. 2013. “Forecasting Liquidity-Adjusted Intraday Value-at-Risk with Vine Copulas.” *Journal of Banking & Finance* 37 (9): 3334–3350.

Xu, Xiaoqing Eleanor, and Hung-Gay Fung. 2005. “Cross-Market Linkages between U.S. and Japanese Precious Metals Futures Trading.” *Journal of International Financial Markets, Institutions and Money* 15 (2): 107–24.

Yang, Kun, Yu Wei, Jianmin He, and Shouwei Li. 2019. “Dependence and Risk Spillovers between Mainland China and London Stock Markets before and after the Stock Connect Programs.” *Physica A: Statistical Mechanics and Its Applications* 526: 120883.

Zhang, Bangzheng, Yu Wei, Jiang Yu, Xiaodong Lai, and Zhenfeng Peng. 2014. “Forecasting VaR and ES of Stock Index Portfolio: A Vine Copula Method.” *Physica A: Statistical Mechanics and Its Applications* 416: 112–124.

Zhang, Dalu. 2014. “Vine Copulas and Applications to the European Union Sovereign Debt Analysis.” *International Review of Financial Analysis* 36: 46–56.

[Dataset] THOMSON REUTERS DATASTREAM, https://www.thomsonone.com/DirectoryServices/2006-04-01/Web.Public/Login.aspx?brandname=datastream

Data Availability Statement

The data that support the findings of this study are openly available in THOMSON

REUTERS DATASTREAM at [https://www.thomsonone.com/DirectoryServices/2006-04-

01/Web.Public/Login.aspx?brandname=datastream], reference number Aluminum (code:

LAHCS00(PS)); Copper (code: LCPCS00(PS)); Nickel (code: LNICS00(PS)); Zinc (code:

LZZCS00(PS)); Lead (code: LEDCS00(PS)).

Appendix A. Test simplifying assumption

Whether the simplifying assumption can be relaxed depends on the given dataset and the tree structure of the vine copula. Recently, Kurz and Spanhel (2017) proposed a new statistical method called the constant conditional correlation (CCC) test to check whether the simplifying assumption is suitable for each conditional bivariate copula in a vine copula. The idea of this test is that if a conditional copula can be represented by an unconditional copula then the correlation coefficient corresponding to a conditional copula is a constant with respect to conditioning variables. Based on this fact, the null hypothesis of this method is:

$$\rho_{\Omega_1} = \cdots = \rho_{\Omega_L} \tag{A.1}$$

where $\rho_{\Omega_i} := Corr\left(U_{j_e|D_e}, U_{k_e|D_e} | \mathbf{U}_{D_e} \in \Omega_i\right)$, $U_{j_e|D_e}$ and $U_{k_e|D_e}$ are conditioned variables in conditional copula. $\mathbf{U}_{D_e}$ is a conditioning variables set. The support Ω_0 of $\mathbf{U}_{D_e}$ is divided by a partition $\Gamma := \{\Omega_1, \dots, \Omega_L\}$, Ω_i is an element in the partition Γ.

Since the vector $\boldsymbol{\gamma}^{(n)}(\Gamma) = (\hat{\rho}^{(n)}_{\Omega_1}, \hat{\rho}^{(n)}_{\Omega_1}, \dots, \hat{\rho}^{(n)}_{\Omega_L})$ is asymptotically normal distributed, i.e.:

$$\sqrt{n}\left(\widehat{\boldsymbol{\gamma}}^{(n)}(\Gamma) - \boldsymbol{\gamma}(\Gamma)\right) \xrightarrow{d} N\left(\mathbf{0}, \boldsymbol{\Sigma}(\Gamma)\right), \quad n \to \infty \tag{A.2}$$

where $\hat{\rho}_{\Omega_i}^{(n)}$, $i = 1,2,\dots,L$ is the sample Pearson coefficients, $\widehat{\boldsymbol{\gamma}}^{(\mathrm{n})}(\Gamma)$ is the vector-valued true conditional correlations, and $\boldsymbol{\Sigma}(\Gamma)$ is the asymptotic variance-covariance matrix. Kurz and Spanhel (2017) further derived a test statistic to test the null hypothesis by using the asymptotic normality of $\widehat{\boldsymbol{\gamma}}^{(\mathrm{n})}(\Gamma)$, and the test statistic is defined as follows:

$$T_n(\Gamma) = \left(\boldsymbol{W}\widehat{\boldsymbol{\gamma}}^{(n)}(\Gamma)\right)^T (\boldsymbol{W}\widehat{\boldsymbol{\Sigma}}^{(n)}(\Gamma)W)^{-1} \left(\boldsymbol{W}\widehat{\boldsymbol{\gamma}}^{(\mathrm{n})}(\Gamma)\right) \qquad \text{(A. 3)}$$

where $\widehat{\boldsymbol{\Sigma}}^{(n)}(\Gamma)$ is the consistent estimator for $\boldsymbol{\Sigma}(\Gamma)$ and $\boldsymbol{W}$ is a well-defined weight matrix (see Kurz and Spanhel, 2017).

Under the null hypothesis and some regular conditions, $T_n(\Gamma)$ converges in distribution to a χ^2 distribution with degree of freedom $L-1$. i.e.

$$nT_n(\Gamma) \xrightarrow{d} {\chi^2}_{L-1}\ , \qquad n \to \infty \qquad \text{(A. 4)}$$

This novel testing procedure can mitigate the curse of dimensions due to the discretizing of the conditioning variable set and the penalty incorporated in the test statistic.

Appendix B. Measure of dependence

Many kinds of dependence measures can be defined based on the copula theory. This paper refers to two dependence measures: Kendall's τ and the indices of tail dependence.

B.1. Kendall's τ

Kendall's τ measures the concordance between two random variables. The higher the concordance between two random variables, the stronger the dependence. In the discrete case, given two random vectors with the same joint distribution and copula function (X_1, Y_1) and (X_2, Y_2), the vectors are said to be concordant if $X_1 > X_2$ whenever $Y_1 > Y_2$, and $X_1 < X_2$, whenever $Y_1 < Y_2$; the vectors are said to be discordant in the opposite case. Kendall's τ measures the difference between the probability of concordance and of the discordance between two independent random vectors.

Definition: Kendall's τ for two random variables X_1 and X_2 with copula $C(u, v)$, is:

$$\tau = 4 \int_0^1 \int_0^1 C(u, v)\, dC(u, v) - 1 \qquad \text{(B. 1)}$$

B.2. The indices of tail dependence

The indices of tail dependence measure the dependence in a tail, or extreme values of two random variables. In particular, there are two kinds of indices: the indices of upper tail dependence and the indices of lower tail dependence.

Definition: X and Y are two continuous random variables, with distribution functions $F_x(.), F_y(.)$. If $C(.,.)$ denotes the copula for X and Y, then:

$$\lambda_L = \lim_{u \to 0} \Pr(F_x(x) \leq u | F_y(.) \leq u) = \lim_{u \to 0} \frac{C(u,u)}{u} \quad \text{(B. 2)}$$

$$\lambda_U = \lim_{u \to 1} \Pr(F_x(x) \geq u | F_y(.) \geq u) = \lim_{u \to 1} \frac{1 - 2u + C(u,u)}{1 - u} \quad \text{(B. 3)}$$

where λ_L and λ_U represent the indices of lower tail dependence and upper tail dependence respectively. λ_L, $\lambda_U \in (0,1)$. If λ_L and λ_U take positive values, there exists tail dependence between the two random variables. The definition of these two measures is independent from the marginal distribution $F_x(.)$, and $F_y(.)$ and only relates to the copula $C(.,.)$.

Appendix C. Bivariate copula families

The vast majority of studies have confirmed the existence of extreme and asymmetric volatility in various financial asset markets. Therefore, we apply several bivariate copulas with

different tail dependence structures to fully capture the tail dependence between the variables considered in this paper.

C.1. Elliptical copula family

The Gaussian copula function is as follows:

$$C^{Gaussian}(u, v; \rho) = \Phi_{\rho}(\Phi^{-1}(u), \Phi^{-1}(v); \rho) \quad (C.1)$$

where $\rho \in (-1,1)$ denotes the linear correlation coefficient between two random variables. Φ_{ρ} is the bivariate normal distribution function. Φ^{-1} is the inverse of the univariate normal distribution function. The Gaussian copula has no tail dependence.

The bivariate Student's *t* copula is as follows:

$$C_{\nu}^{student-t}(u, v; \rho) = t_{\rho\,\nu}(t^{-1}(u), t^{-1}(v); \rho) \quad (C.2)$$

where $\rho \in (-1,1)$ denotes the linear correlation coefficient between two random variables. $t_{\rho\,\nu}$ is the bivariate t-distribution function with linear correlation coefficient ρ and the degree of freedom ν. t^{-1} is the inverse of the univariate t-distribution function. The t-copula exhibits symmetrical tail dependence.

C.2. Archimedean copula family

The bivariate Archimedean copula function is:

$$\mathrm{C}(u_1, u_2) = \varphi^{[-1]}(\varphi(u_1) + \varphi(u_2)) \qquad (\mathrm{C}.3)$$

where $\varphi: [0,1] \rightarrow [0,\infty]$ is a continuous strictly decreasing convex such that $\varphi(1) = 0$ and $\varphi^{[-1]}$ is the pseudo-inverse φ as follows:

$$\varphi^{[-1]} = \begin{cases} \varphi^{-1}(t), & 0 \leq t \leq \varphi(0) \\ 0, & \varphi(0) \leq t \leq \infty \end{cases} \qquad (\mathrm{C}.4)$$

Table C1 presents some properties of the Clayton, Gumbel, Frank, and BB1 copulas that belong to the bivariate Archimedean copula families. We can see from Table C1 that the Frank-copula has no tail dependence, the Gumbel-copula exhibits asymmetrical lower tail dependence, and the BB1 copula has asymmetrical upper dependence.

Table C1. Properties of some Archimedean copula families

Name	*Function*	*Para.range*	*Kendall's* τ	*Tail.dep. (l.u.)*
Frank	$-\log\left(\frac{e^{-\theta t}-1}{e^{-\theta}-1}\right)$	$\theta \in \Re$	$1-\frac{4}{\theta}+\frac{D_1(\theta)}{\theta}$	(0,0)
BB8	$-\log\left(\frac{1-(1-\delta t)^{\theta}}{1-(1-\delta)^{\theta}}\right)$	$\theta \geq 1, \delta \in (0,1]$	$g(\delta,\theta)$	$(2^{-\frac{1}{\delta}}, 2-2^{\frac{1}{\theta}})$
Gumbel	$(-\log t)^{\theta}$	$\theta \geq 1$	$1-\frac{1}{\theta}$	$(2, 2-2^{\frac{1}{\theta}})$
BB1	$(t^{-\theta}-1)^{-\delta}$	$\theta > 0, \delta \geq 1$	$1-\frac{2}{\delta(\theta+2)}$	$(2^{-\frac{1}{\theta\delta}}, 2-2^{\frac{1}{\theta}})$
Clayton	$\frac{1}{\theta}(t^{-\theta}-1)$	$\theta > 0$	$\frac{\theta}{(\theta+2)}$	$(2^{-\frac{1}{\theta}})$

Note: $D_1(\theta)=\int_0^{\theta}\frac{c/\theta}{exp(x)-1}dx$ is Debye function. ***Para.range*** represents the range of parameters in copula function. $g(\delta,\theta)=1+\frac{4}{\delta\theta}\int_0^1(-(1-(1-t)^{\theta}))^{\delta+1}\times\frac{(1-(1-t)^{\theta})^{\delta+1}-1}{(1-t)^{\theta-1}})dt$. ***Tail.dep. (l.u.)*** denotes the values of lower and upper tail dependence indices.

C.3. Survival copula

A survival copula is a special rotated-copula function. The rotation of the copula greatly enriches the types of copulas and enables them to better capture the dependence. A copula function which is rotated 180 degrees is called the survival copula of the original：

$$C_{180}(u_1,u_2)=u_1+u_2-1+C(1-u_1,1-u_2) \tag{C.5}$$

In contrast, the Gumbel copula has an asymmetrical upper tail dependence, while the BB1 copula exhibits an asymmetrical lower tail dependence.

Appendix D. Results for marginal distribution modelling

The parameters estimation and statistical tests for the GARCH (1,1) model in Period 1 are listed in Table D1. The Lagrange Multiplier test for almost all non-ferrous metal futures strongly reject the null hypothesis at lag 3, 5, and 7 at 5% significance level, except zinc, whose Lagrange Multiplier test reject the null hypothesis at lag 3 at the 1% significance level. In general, this evidence implies no heteroscedasticity in standardized residuals generated by marginal models. The Ljung-Box test for all five non-ferrous metal futures cannot reject the null hypothesis of no autocorrelation at lag 1, 2, and 5 at 5% significance level, which indicates no autocorrelation in standardized residuals generated by marginal models. The Sign Bias test for all five non-ferrous metal futures cannot reject the null hypothesis of no positive/negative volatility response at the 5% significance level. The above statistical results demonstrate that the GARCH (1,1) model is adequate for modelling marginal distributions of all five non-ferrous metal futures in Period 1 and there is no need to further employ asymmetrical GARCH models.

Table D2 lists estimations and statistical tests for GARCH (1,1) model in Period 2. The Ljung-Box test for each marginal model cannot reject the null hypothesis of no autocorrelation

Table D1. Parameter estimates and statistical tests for GARCH (1,1) in Period 1

Parameter	AL		CU		NIC		ZINC		LEAD	
	Est./Stat.	*p*-value	Est./Stat.	*p*-value	Est./Stat.	*p*-value	Est./Stat.	*p*-value	Est./Stat.	*p*-value
μ	0.1811	0.1402	0.3989	0.0205	0.4547	0.0789	0.2800	0.1507	0.3337	0.1178
ω	0.1052	0.2479	0.2509	0.2324	1.0839	0.2663	0.1431	0.3917	0.3219	0.3632
α	0.1196	0.0008	0.1007	0.0057	0.0909	0.0337	0.0826	0.0012	0.1056	0.0054
β	0.8775	0.0000	0.8841	0.0000	0.8743	0.0000	0.9163	0.0000	0.8934	0.0000
D.O.F.	63.2675	0.6779	35.976	0.5642	18.1901	0.3132	22.453	0.4182	7.1101	0.0119
AIC	4.8044		5.2886		6.1072		5.6796		5.8762	
Logli.	-823.766		-907.2917		-1048.485		-974.7371		-1008.652	
LB test:										
lags	Est./Stat.	*p*-value	Est./Stat.	*p*-value	Est./Stat.	*p*-value	Est./Stat.	*p*-value	Est./Stat.	*p*-value
1	0.9517	0.3293	0.0159	0.8996	1.780	0.1821	0.6824	0.4088	1.794	0.1805
2	1.6392	0.3303	0.2999	0.7957	1.784	0.3013	1.0589	0.4795	2.020	0.2594
5	2.2473	0.5612	1.8065	0.6648	2.043	0.6082	1.8167	0.6623	3.574	0.3122
LM test:										
lags	Est./Stat.	*p*-value	Est./Stat.	*p*-value	Est./Stat.	*p*-value	Est./Stat.	*p*-value	Est./Stat.	*p*-value
3	4.262	0.0389	0.0005	0.9823	0.0426	0.8364	0.0172	0.8957	0.4738	0.4912
5	4.763	0.1166	0.5035	0.8826	0.9862	0.7370	2.0818	0.4534	2.3869	0.3919
7	5.556	0.1740	1.7694	0.7660	5.7696	0.1575	4.2383	0.3135	2.7874	0.5546
SB test:										
	Est./Stat.	*p*-value	Est./Stat.	*p*-value	Est./Stat.	*p*-value	Est./Stat.	*p*-value	Est./Stat.	*p*-value
Negative	0.9484	0.3436	1.503	0.1336	1.1321	0.2584	0.0129	0.9897	0.0677	0.9461
Positive	0.8263	0.4092	1.878	0.0613	0.8907	0.3737	0.9327	0.3517	1.6953	0.0909

Note: **AL**: Aluminum, **CU**: Copper, **NIC**: Nickel, **ZINC**: Zinc, **LEAD**: Lead. Est./Stat. denotes estimated parameters or statistics. Shape is the degree of freedom for the fitted *t*-distribution. Logli. denotes log-likelihood value. **LB test** represents the Ljung-Box test. **LM test** represents the Lagrange Multiplier test. **SB test** represents Sign Bias test. Negative /Positive show the results of negative sign bias test and positive sign bias test respectively. μ、ω、α_1、β_1 are estimated coefficients in equation (4.1) and (4.2). AIC is the value of Akaike information criterion. Lags denotes the lag-order of corresponding statistical test.

at lag 1, 2, and 5 at 5% significance level, which indicates no autocorrelation in standardized residuals generated by the marginals. The Lagrange Multiplier test applied to each marginal

Table D2. Parameter estimates and statistical tests for GARCH (1,1) in Period 2

Para.	AL		CU		NIC		ZINC		LEAD	
	Est./Stat.	*p*-value	Est./Stat.	*p*-value	Est./Stat.	*p*-value	Est./Stat.	*p*-value	Est./Stat.	*p*-value
μ	-0.1221	0.5067	0.1147	0.4973	-0.0917	0.7020	0.1057	0.6159	0.1111	0.6474
ω	0.0000	0.9996	0.0673	0.6762	0.1789	0.4758	0.0000	0.9999	0.1579	0.4895
α	0.0249	0.5505	0.0827	0.0321	0.0509	0.0980	0.0403	0.0599	0.0660	0.0530
β	0.9713	0.0000	0.9114	0.0000	0.9356	0.0000	0.9543	0.0000	0.9233	0.0000
D.O.F.	9.6752	0.0427	5.1026	0.0002	7.3833	0.0066	12.5992	0.1285	13.2814	0.1341
AIC	5.3061		5.4710		5.9947		5.7297		6.0093	
Logli.	-745.8194		-769.1506		-843.2555		-805.7528		-845.3103	
LB test:										
lags	Est./Stat.	*p*-value	Est./Stat.	*p*-value	Est./Stat.	*p*-value	Est./Stat.	*p*-value	Est./Stat.	*p*-value
1	0.2502	0.6169	0.1817	0.6699	0.0299	0.8628	0.6586	0.4170	0.3757	0.5399
2	0.2570	0.8201	1.1513	0.4517	0.3110	0.7896	1.0177	0.4925	0.4361	0.7244
5	0.7903	0.9050	2.3848	0.5307	0.9836	0.8634	3.5930	0.3094	2.8267	0.4396
LM test:										
lags	Est./Stat.	*p*-value	Est./Stat.	*p*-value	Est./Stat.	*p*-value	Est./Stat.	*p*-value	Est./Stat.	*p*-value
3	0.9536	0.3288	0.1180	0.7312	1.5550	0.2124	0.6959	0.4041	0.0065	0.9357
5	1.2101	0.6718	1.8260	0.5111	2.7820	0.3230	1.3908	0.6215	0.9486	0.7482
7	4.7716	0.2487	4.5460	0.2746	3.6360	0.4021	5.5490	0.1746	2.8856	0.5354
SB test										
	Est./Stat.	*p*-value	Est./Stat.	*p*-value	Est./Stat.	*p*-value	Est./Stat.	*p*-value	Est./Stat.	*p*-value
Negative	0.6904	0.4905	0.2111	0.8329	1.2140	0.2258	1.5849	0.1141	0.3984	0.6906
Positive	1.0252	0.3062	1.0054	0.3156	1.7750	0.0769	0.7931	0.4284	0.3686	0.7127

Note: **AL**: Aluminum, **CU**: Copper, **NIC**: Nickel, **ZINC**: Zinc, **LEAD**: Lead. Est./Stat. denotes estimated parameters or statistics. *D.O.F.* is the degree of freedom for the fitted *t*-distribution. Logli. denotes log-likelihood value. **LB test** represents the Ljung-Box test. **LM test** represents the Lagrange Multiplier test. **SB test** represents Sign Bias test. Negative /Positive show the results of negative sign bias test and positive sign bias test respectively. μ、ω、α_1、β_1 are estimated coefficients in equation (4.1) and (4.2). AIC is the value of Akaike information criterion. Lags denotes the lag-order of corresponding statistical test.

model cannot reject the null hypothesis at lag 3, 5, and 7 at 5% significance level, which implies no heteroscedasticity in standardized residuals generated by the marginals. The positive and negative Sign Bias test for all five non-ferrous metal futures cannot reject the null hypothesis of no asymmetry volatility response at the 5% significance level. Therefore, the GARCH (1,1) is also adequate for modelling the marginal distributions of all five non-ferrous metal futures in Period 2 and there is still no need to use asymmetrical GARCH model.

Table D3 shows estimations and statistical tests for GARCH (1,1) model in Period 3. Similar to the previous two periods, the results of Ljung-Box test for each marginal model indicate no autocorrelation in standardized residuals generated by the marginals. The Lagrange Multiplier test applied to each marginal model still cannot reject the null at lag 3, 5, and 7 at 5% significance level, which also implies no heteroscedasticity in standardized residuals generated by the marginals. The results of positive and negative Sign Bias test for all five non-ferrous metal futures documents no asymmetry volatility response at 5% significance level. Thus, the GARCH (1,1) is adequate for modelling the marginal distributions of all five non-ferrous metal futures in Period 3 and there is still no need to use asymmetrical GARCH model.

The goodness-of-fit for Student's *t* innovations in the marginal models are evaluated by

Table D3. Parameter estimates and statistical tests for GARCH (1,1) in Period 3

Parameter	AL		CU		NIC		ZINC		LEAD	
	Est./Stat.	*p*-value	Est./Stat.	*p*-value	Est./Stat.	*p*-value	Est./Stat.	*p*-value	Est./Stat.	*p*-value
μ	-0.0306	0.8151	-0.1023	0.4512	-0.0117	0.9586	0.0369	0.8288	-0.1259	0.4176
ω	0.7426	0.5302	0.1655	0.4353	0.0475	0.7424	0.2518	0.3649	0.2376	0.3077
α	0.0873	0.1435	0.0362	0.1184	0.0000	1.0000	0.0272	0.1934	0.0379	0.1071
β	0.7859	0.0017	0.9382	0.0000	0.9972	0.0000	0.9471	0.0000	0.9395	0.0000
D.O.F.	12.1884	0.0480	10.1384	0.0638	99.3540	0.7802	80.9365	0.7281	6.3735	0.0080
AIC	4.5993		4.6726		5.5985		5.0765		4.9967	
Logli.	-703.2854		-714.5843		-857.1674		-776.7853		-764.4905	
LB test:										
lags	Est./Stat.	*p*-value	Est./Stat.	*p*-value	Est./Stat.	*p*-value	Est./Stat.	*p*-value	Est./Stat.	*p*-value
1	0.1413	0.7070	0.1699	0.6802	0.3878	0.5335	0.0087	0.9257	1.3070	0.2530
2	1.7817	0.3017	0.1901	0.8603	0.9845	0.5033	0.1004	0.9194	1.5080	0.3591
5	5.3702	0.1260	2.5819	0.4887	2.0614	0.6040	1.5022	0.7394	2.9370	0.4187
LM test:										
lags	Est./Stat.	*p*-value	Est./Stat.	*p*-value	Est./Stat.	*p*-value	Est./Stat.	*p*-value	Est./Stat.	*p*-value
3	0.0003	0.9872	1.3270	0.2493	1.1550	0.2826	1.0920	0.2960	0.1178	0.7315
5	0.7154	0.8188	2.7040	0.3358	1.8170	0.5131	1.4470	0.6064	0.3003	0.9402
7	1.0222	0.9099	4.5270	0.2769	4.2650	0.3100	1.8350	0.7521	0.6094	0.9674
SB test:										
	Est./Stat.	*p*-value	Est./Stat.	*p*-value	Est./Stat.	*p*-value	Est./Stat.	*p*-value	Est./Stat.	*p*-value
Negative	0.1502	0.8807	0.7693	0.4423	2.0139	0.0449	0.5283	0.5977	0.1304	0.8963
Positive	0.7614	0.4470	0.4060	0.6850	0.1905	0.8491	0.4434	0.6578	0.2806	0.7792

Note: **AL**: Aluminum, **CU**: Copper, **NIC**: Nickel, **ZINC**: Zinc, **LEAD**: Lead. Est./Stat. denotes estimated parameters or statistics. Shape is the degree of freedom for the fitted *t*-distribution. Logli. denotes log-likelihood value. **LB test** represents the Ljung-Box test. **LM test** represents the Lagrange Multiplier test. **SB test** represents Sign Bias test. Negative /Positive show the results of negative sign bias test and positive sign bias test respectively. μ、ω、α_1、β_1 are estimated coefficients in equation (4.1) and (4.2). AIC is the value of Akaike information criterion. Lags denotes the lag-order of corresponding statistical test.

Kolmogorov-Smirnov (KS) test and Cramer-von Mises (CvM) test. The results are summarized in Table D4. We find that KS test and CvM test for aluminum, copper, nickel, zinc and lead in

three periods fail to reject the null hypothesis at 5% level. This evidence suggests that Student's *t* distributed model is a suitable model for marginal distributions. As Dißmann et al. (2013) has suggested that the innovation distribution is hard to identify. Rigorously, we follow them to transform the standardized residuals generated by the GARCH model into marginally uniform data by using the empirical PIT, rather than the parametric one.

Table D4. Goodness-of-fit test results for Student's *t* innovations in three periods

	*Period 1**: Jan, 2002- Aug, 2008***		*Period 2**: Aug, 2008- Jan, 2014***		*Period 3**: Jan, 2014- Dec, 2019***	
	***CvM** p-value*	***KS** p*-value	***CvM** p*-value	***KS** p*-value	***CvM** p*-value	***KS** p*-value
AL	0.6784	0.7466	0.5659	*0.6901*	0.5041	0.6267
CU	0.1766	0.1715	0.0626	0.0721	0.3382	0.4103
NIC	0.6630	0.8375	0.3752	0.4865	0.7284	0.7110
ZINC	0.4147	0.5516	0.4673	0.4227	0.9091	0.8746
LEAD	0.0928	0.0847	0.6089	0.5421	0.0965	0.0847

Note: **AL**: Aluminum, **CU**: Copper, **NIC**: Nickel, **ZINC**: Zinc, **LEAD**: Lead. **KS-stat.** denotes the Kolmogorov-Smirnov statistics. ***KS** p*-value denotes the *p*-value of the Kolmogorov-Smirnov statistical test. ***CvM** p*-value denotes the *p*-value of the Cramer-von Mises statistical test.